Progress in Oceanography 160 (2018) 167–185

Contents lists available at ScienceDirect

Progress in Oceanography

journal homepage: www.elsevier.com/locate/pocean

Unraveling the intricate dynamics of planktonic Arctic marine food webs. A sensitivity analysis of a well-documented food web model

Blanche Saint-Béat*, Frédéric Maps, Marcel Babin

Takuvik Joint International Laboratory, Laval University (Canada) – CNRS (France), Département de biologie et Québec-Océan, Université Laval, Quebec, Quebec, Canada

ARTICLE INFO

Keywords:
Food web
Sensitivity analysis
Ecosystem functioning
ENA
Linear inverse modeling
Arctic
Amundsen Gulf

ABSTRACT

The extreme and variable environment shapes the functioning of Arctic ecosystems and the life cycles of its species. This delicate balance is now threatened by the unprecedented pace and magnitude of global climate change and anthropogenic pressure. Understanding the long-term consequences of these changes remains an elusive, yet pressing, goal. Our work was specifically aimed at identifying which biological processes impact Arctic planktonic ecosystem functioning, and how. Ecological Network Analysis (ENA) indices reveal emergent ecosystem properties that are not accessible through simple *in situ* observation. These indices are based on the architecture of carbon flows within food webs. But, despite the recent increase in *in situ* measurements from Arctic seas, many flow values remain unknown. Linear inverse modeling (LIM) allows missing flow values to be estimated from existing flow observations and, subsequent reconstruction of ecosystem food webs. Through a sensitivity analysis on a LIM model of the Amundsen Gulf in the Canadian Arctic, we were able to determine which processes affected the emergent properties of the planktonic ecosystem. The analysis highlighted the importance of an accurate knowledge of the various processes controlling bacterial production (e.g. bacterial growth efficiency and viral lysis). More importantly, a change in the fate of the microzooplankton within the food web can be monitored through the trophic level of mesozooplankton. It can be used as a "canary in the coal mine" signal, a forewarner of larger ecosystem change.

1. Introduction

Extreme conditions and high seasonality prevailing in the Arctic Ocean have shaped many aspects of ecosystem functioning, species diversity and life history traits. The most obvious examples of extreme conditions are sub-zero water temperatures and the drastic seasonal alternation between sea-ice covered and open waters, and between polar night and midnight sun. The phytoplanktonic primary producers are at the basis of the pelagic arctic food web. Phytoplankton growth and abundance are determined by ice coverage and photoperiod coupled with the upward supply of inorganic nutrients; their extreme dynamics causes strong seasonal changes in the availability of food supply for phytoplankton consumers. Arctic zooplankton, which are dominated by copepods, occupy a key position between phytoplankton and higher trophic levels. Arctic copepods have evolved a strong seasonal life-cycle strategy: while they winter at depth, they migrate upwards in spring and reproduce in summer, matching the seasonal dynamics of phytoplankton production (Maps et al., 2013). In this way copepods can convert primary organic biomass, mainly produced during the short polar spring and summer, into large energy-rich lipid stores (up to 70% of their body weight) that are subsequently available all year long for their predators (Darnis et al., 2012). For this reason, they are the linchpin of energy transfer through the entire Arctic marine ecosystem (Darnis et al., 2012).

The Arctic is the area of the planet that is the most affected by global warming (Walsh, 2008). One of the most striking and immediate consequences of the steady rise in temperature over the Arctic Ocean has been the decrease of the seasonal sea ice extent and thickness together with the progressive disappearance of multiannual sea ice in the central Arctic (Kwok and Rothrock, 2009). These on-going changes affect the light field and the nutrient supply from deeper layers of the water column (Wassmann et al., 2011) and, hence, have dramatic consequences for both sea ice (sympagic) and water column (pelagic) ecosystems. They directly affect phytoplankton seasonal growth (Ardyna et al., 2014; Arrigo et al., 2008), which can potentially have an important impact on Arctic marine food webs. Additionally, in the wake of Arctic Ocean physico-chemical perturbations, changes in biodiversity have already been observed at different trophic levels, from phytoplankton to fish (Gaston et al., 2003; Li et al., 2009). The consequences of these numerous and drastic changes at short-, medium- and long-

* Corresponding author.
E-mail address: blanche.saint-beat@takuvik.ulaval.ca (B. Saint-Béat).

https://doi.org/10.1016/j.pocean.2018.01.003
Received 25 July 2017; Received in revised form 2 December 2017; Accepted 9 January 2018
Available online 11 January 2018
0079-6611/ © 2018 Elsevier Ltd. All rights reserved.

term time scales remain mostly unknown.

Food webs materialize the transfer of energy and matter between organisms that eat others and/or are themselves eaten depending on their trophic level (Pimm, 1984). Because living communities are mainly organised according to feeding behaviour (Elton, 1927), food webs integrate essential information about population dynamics, community structure, species interactions and community stability (Link et al., 2005). Environmental changes impacting any component of a food web can trigger reorganisation, which itself can cause larger effects such as changes in ecosystem performance (e.g. Ayers et al., 2013; Chrystal and Scharler, 2014; Naeem et al., 1994) or modifications in biogeochemical cycles (e.g. Carstensen et al., 2014; Loreau, 1994; Riemann et al., 2016). Food webs are characterized by the way flows of energy and matter are organised. They define peculiar structural and functional features of an ecosystem, so-called 'emergent properties', which are specific to an ecosystem in given environmental conditions. A change in environmental conditions can lead to a modification in the structure and organisation of energy and matter pathways and, consequently, in ecosystem properties. Numerical indices, resulting from Ecological Network Analysis (ENA), reveal emergent ecosystem properties and allow us to distinguish the different states an ecosystem goes through due to either natural evolution or environmental change (Baird et al., 2007). Interpretation of ENA indices also inform on the potential of ecosystems for stability (Saint-Béat et al., 2015). Stability is the capacity of an ecosystem to maintain its state over time, independent of the nature of perturbations it undergoes. Therefore, an accurate knowledge of food web features and its ENA indices is essential for (i) determining whether an ecosystem will be able to maintain its current degree of functioning and the services it provides in face of anthropogenic perturbations, and (ii) characterizing and monitoring diverse ecosystem changes over a broad spatio-temporal range.

In Arctic ecosystems, environmental changes are essentially filtered and transferred to higher trophic levels of the pelagic food-web via plankton (Beaugrand and Kirby, 2010). In this context, a thorough understanding of the functioning of planktonic food webs is crucial for determining the states of stability of Arctic pelagic ecosystems and tracking their evolution. Unfortunately, monitoring of the Arctic pelagic ecosystem based on food web reconstruction and ENA calculations is limited by the current lack of data. This bottleneck is due to constrained access to the Arctic Ocean because of challenging and costly logistics and a narrow time window for in-situ measurements, which is restricted to late spring and summer for most ice-breakers. Nevertheless, missing data can be estimated by mathematical approaches such as the Linear Inverse Modeling (LIM). LIM allows for unknown food web flows to be estimated from *in situ* measurements and literature (Vézina and Platt, 1988).

The overarching objective of the present work was to use a well-documented food web model (i.e. LIM) to better understand the heterotrophic processes that shape the carbon distribution throughout food web and thus the functioning of Arctic ecosystems. In a context of rapid climate change, these processes are the key elements that sustain ecosystem functioning and services. We performed a sensitivity analysis on an existing Amundsen Gulf food web model (Forest et al., 2011b). Data about individual processes were removed one at a time to mimic the impacts of a potential lack of information on the model output. We identified critical information that had major impact on the emergent properties of Arctic pelagic ecosystems: processes regulating bacterial production and the fate of microzooplankton production. This crucial information should guide future field sampling and lead to a better description and more effective monitoring of Arctic pelagic ecosystems.

2. Material and methods

2.1. Study area

The Amundsen Gulf is a large channel (approximately 60,000 km^2) connecting the southeast Beaufort Sea to the Canadian Archipelago. Three water masses co-occur in the region: the Polar-Mixed Layer (PML) on top, the intermediate Pacific Halocline (PH) and the Atlantic Layer (AL) in the deepest part of the Gulf. Oceanic circulation is variable in the region and is not completely understood (Barber et al., 2010). Seasonal sea ice forms at the beginning of October near the coast and by late December the sea ice cover is usually consolidated over the entire region. The ice begins to break up in early June when wind conditions and surface circulation are suitable to open the Cape-Bathurst polonya, pushing the ice away from the Gulf.

2.2. Linear Inverse Modeling using Monte Carlo Markov chain (LIM-MCMC)

2.2.1. Principle

Linear inverse modeling (LIM) is a method emanating from physical oceanography. It was first applied to ecology by Vézina and Platt (1988) and has often been used since then to estimate carbon flows through marine food webs (e.g. Breed et al., 2004; Marquis et al., 2007; Savenkoff et al., 2001; Vézina and Pace, 1994). LIM combines a map of the food web (i.e. topology) and a set of constraints on processes corresponding to a particular flow (e.g. respiration) and /or to a sum of flows (e.g. consumption by a particular biological compartment). Topology and constraints are determined from *in situ* data and literature, in order to estimate a value for each flow of the food web (Fig. A1). In this way, a snapshot of the quantity of carbon involved in each flow is obtained. To simplify the model and reduce the calculation time, species are grouped in numerical compartments according to their general features such as size, diet and trophic behaviour, etc. All trophic interactions that exist between the resulting compartments are mapped, and physiological processes essential for mass-balance computation, such as respiration, egestion or exudation (if applicable), are added for each living compartment. Mass-balance is the balance between inflows (i.e. ingestion) and outflows (e.g. export, respiration) for each compartment. The LIM approach is based on one assumption: compartment biomasses are constant. Consequently, mass-balances are at the equilibrium (i.e. equal to zero). Mass-balances are integrated to the LIM model as linear equations; they constitute the first constraints. They are completed by two types of constraints: (1) equalities that constrains flows to a single value, corresponding to the average of *in situ* values (hereafter "hard constraints") (Fig. A1) and (2) pairs of inequalities that define the lower and upper limits of the flows (hereafter "soft constraints") (Fig. A1). These 'soft' constraints extracted from both the literature and *in situ* measurements, limit flows to a range of realistic values. The integration of *in situ* data as range of constraints, allows considering the uncertainty of measurements. The complementarity of 'hard' and 'soft' constraints combination brings flexibility to the model, providing several possible solutions for each flow, defined in a solution space (Fig. A1). The exploration of this solution space has evolved since the application of LIM to the ecology field. At first, the minimisation of the sum of squared flow values was considered as the single solution of flows meaning that, this way, a single food web is created (Vézina and Platt, 1988). This approach was used in many studies, including that of Forest et al. (2011b) (see Section 2.2.2. below). More recently, this method was coupled with a random sampling method, the Monte Carlo Markov Chain (MCMC). This combination allows a set of solutions to be calculated for each flow (Van den Meersche et al., 2009; van Oevelen et al., 2010), and thus, to explore the full solution space (Fig. A1 in appendix) and to propose different values for each flow. Ultimately, several realistic food webs, fulfilling all constraints, are obtained.

2.2.2. Model structure

The model used in this study was derived from an existing food web model (Forest et al., 2011b).

Forest et al.'s model describes the planktonic food web of the Amundsen Gulf in spring-summer 2008 between surface and 395-m

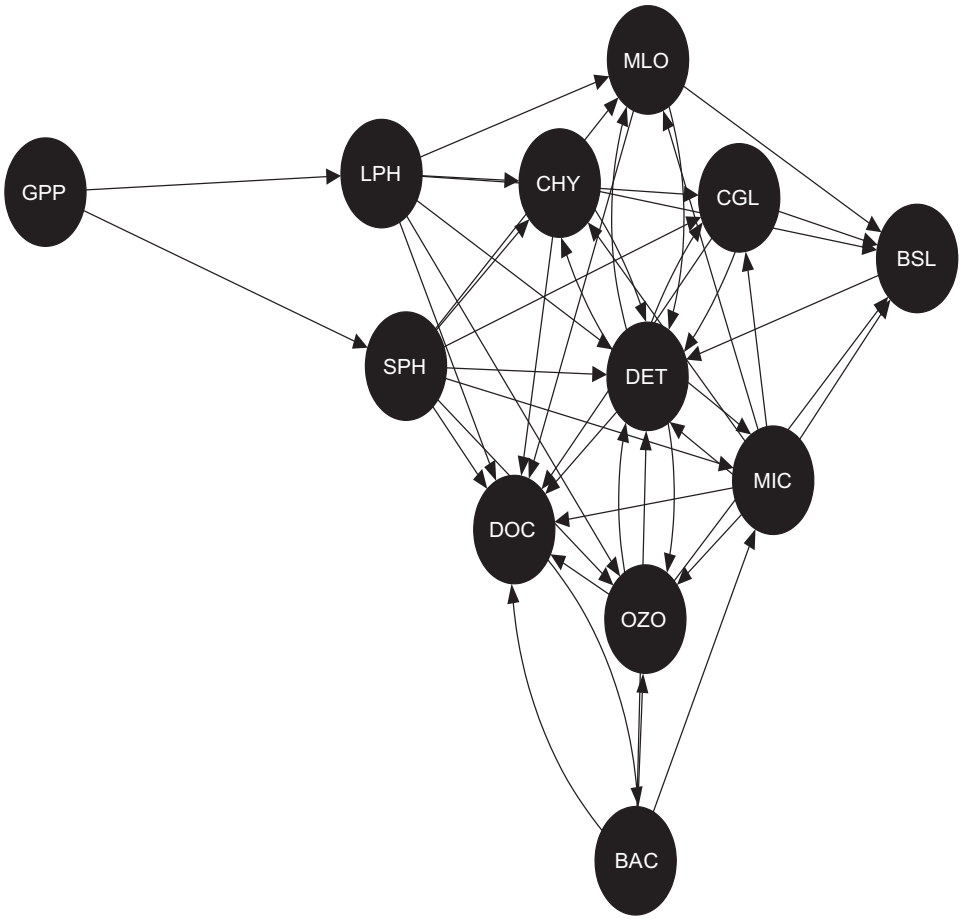

Fig. 1. Food web diagram representing only internal flows (n = 44). GPP = growth primary production, LPH = large phytoplankton, SPH = small phytoplankton, BAC = bacteria, MIC = microzooplankton, BSL = *Boreogadus saida* larvae, OZO = other zooplankton, MLO = *Metridia longa*, CHY = *Calanus hyperboreus*, CGL = *Calanus glacialis*. A list of all flow (including respiration and export) is available in Appendix in Table A1.

deep. The carbon entry is strictly constrained by the annual value of GPP for small and large phytoplankton. This carbon flows through the food web until it is lost by respiration, sinks to depth or is exported (residual flows). The sedimentation of carbon at 395 m was estimated from long-term traps deployed during the period considered. The residual carbon flows were adjusted from the net community production. They correspond to the part of carbon consumed by compartments that are not integrated in this model.

In the present study, the biological compartments, from phytoplankton to mesozooplankton, were complemented with a new compartment for Arctic cod larvae, defined as *young of the year* (age-0) (Fig. 1). The level of aggregation chosen is the best that can be reached with respect to the available *in situ* data. The set of constraints (hard and soft constraints) on flows, expressed in gC m^{-2} over the entire spring-summer period, was enriched with metabolic rates and allometric relations (see bold parameters in Table 1). As a consequence, 11 compartments, 65 flows, 13 hard constraints (11 mass balances and 2 equalities on primary production) as well as 132 soft constraints were considered in our model. In this model, only GPP of small and large phytoplankton was integrated as hard constraints while others field measurements were integrated to the model as lower and upper limits of soft constraints considering 95% confidence interval for each process in order to account for the natural variability observed *in situ*.

2.2.3. Data

The constraints used in Forest et al.'s model and the present study are supported by a large set of field measurements (Table 1). All measurements were conducted during the Circumpolar Flaw Lead (CFL) field campaign in spring-summer 2008. Details about the measurements were described in Forest et al. (2011b) and only a summary of original *in situ* data and the new elements are described here.

2.2.3.1. Phytoplankton. The total gross primary production was estimated from the new and the regenerated production. First the new production was estimated using the DIC: NO_3^- depletion ratio recorded *in situ* in the 0–80 m water layer. The nitrogen uptake by phytoplankton was measured via a classical 15 N labeling method as described in Tremblay et al. (2006). Then the proportion of NO_3^- uptake on the total N uptake allowed to calculate the *f*-ratio as defined by Dugdale and Goering (1967) for each station. Gross primary production (GPP) was then estimated by dividing the new production by the *f*-ratio. The chl *a* biomass of each fraction was converted into carbon biomass using the mean C: chl *a* conversion factor of 59.3 (Forest et al., 2011b). The relative proportions of ice algae and phytoplankton were applied to the previously determined GPP in order to estimate their contribution to the GPP.

2.2.3.2. Pelagic bacteria. Vertical profiles of bacterial production were obtained with the ^{3}H-leucine incorporation method (Smith and Azam, 1992). Bacterial production was converted into carbon units using a conversion factor of 1.5 kgC per mol of ^{3}H-Leucine (Garneau et al., 2008). Extracellular enzyme activity (EEA), which represents the sum of protease and carbohydrase exoenzymatic activities, was used to constrain degradation of detritus to DOC and to constrain exudation of DOC by bacteria. Moreover, the part of bacterial production lost by viral lysis (i.e. to DOC) was assumed to range from 7% to 52% (Wilhelm and Suttle, 1999).

2.2.3.3. Particulate organic carbon. Vertical fluxes of particulate carbon were estimated via long-term sampling using an automated sediment trap deployed at 104 m (from November 2007 to August 2008) and via short-term sampling by interceptor traps deployed for 24 h at 50, 100 and 150 m depths at several stations in June and July 2008. Samples

Table 1
Parameters integrated to the model as hard or soft constraints. Parameters are characterized by their origin. Bold parameters correspond to new information integrated into the model in this study. AE = Assimilation Efficiency = (Ingestion-Egestion)/Ingestion, GGE = Gross Growth Efficiency = Production/Ingestion and Production = Ingestion-Egestion-Exudation-Respiration OR Production = Predation on the considered compartment + export, BGE = Bacterial Growth Efficiency = BP/(BP + BR). Model number refers to the model number for which the information about the parameter was removed (for more details see Table A2).

Parameter	What is it?	Reference	Model number
HARD CONSTRAINTS:			
Gross primary production	*In situ* data	Forest et al. (2011b)	–
SOFT CONSTRAINTS:			
Phytoplankton: divided in two groups			
Respiration	Metabolic rate	Vézina and Platt (1988)	–
Exudation	Metabolic rate	Gosselin et al. (1997) and Klein et al. (2002)	–
Mesozooplankton: divided in four groups			
Production	*In situ* data	Forest et al. (2011b)	1-2-3-4
Herbivory by each group (except one)	*In situ* data	Forest et al. (2011b)	7-8-9
Total respiration	*In situ* data	Forest et al. (2011b)	10
Respiration minimal	**Metabolic rate**	Vézina and Pace (1994)	–
Respiration maximal	**Allometric relation**	Moloney and Field (1989)	25-26-27-28
Ingestion maximal	**Allometric relation**	Moloney and Field (1989)	31-32-33-34
AE	Metabolic rate	Daly (1997) and Frangoulis et al. (2010)	–
GGE	Metabolic rate	Frangoulis et al. (2010) and Straile (1997)	–
Excretion	Metabolic rate	Vézina and Platt (1988)	–
Microzooplankton			
Production	*In situ* data	Forest et al. (2011b)	5
Bacterivory	*In situ* data	Forest et al. (2011b)	11
Herbivory and detritivory	*In situ* data	Forest et al. (2011b)	12
Respiration minimal	**Metabolic rate**	Vézina and Pace (1994)	–
Respiration maximal	**Allometric relation**	Moloney and Field (1989)	29
Ingestion maximal	**Allometric relation**	Moloney and Field (1989)	35
AE	Metabolic rate	Vézina and Platt (1988)	–
GGE	Metabolic rate	Straile (1997)	–
Exudation	Metabolic rate	Vézina and Platt (1988)	–
Bacteria			
Production	*In situ* data	Forest et al. (2011b)	6
BGE	Metabolic rate	Forest et al. (2011b)	14
Exudation + viral lysis	*In situ* data	Forest et al. (2011b)	15
Respiration minimal	**Metabolic rate**	Vézina and Pace (1994)	–
Respiration maximal	**Allometric relation**	Moloney and Field (1989)	30
Ingestion maximal	**Allometric relation**	Moloney and Field (1989)	36
Detritus: divided in two groups			
Detritus degradation	*In situ* data	Forest et al. (2011b)	13
Sedimentation	*In situ* data	Forest et al. (2011b)	16
Arctic cod larvae			
Consumption	**Allometric relation**	Hop et al. (1997)	18
Respiration	**Allometric relation**	Hop and Graham (1995)	17
Diet proportion	***In situ* data**	Bouchard et al. (2014)	19-20-21-22-23
AE	**Metabolic rate**	Hop et al. (1997)	–
GGE	**Metabolic rate**	Hop et al. (1997)	–
NCP	*In situ* data	Shadwick et al. (2011)	24

were filtered and analyzed for total particulate carbon (TPC). A portion of the long-term samples were exposed to concentrated HCI fumes for 12 h to remove the inorganic carbon fraction for determination of particulate organic carbon (POC).

2.2.3.4. Microzooplankton. Microzooplankton was composed of two groups: (1) copepods nauplii (size range 50–200 µm) and (2) protozoans of 0.2–5 µm and > 5 µm, that were otherwise sampled and treated. Copepods nauplii were collected using a 10 cm diameter net with a 50 µm mesh size. Nauplii abundance was transformed into carbon biomass according to the carbon content length and width relationship described in (Nozais et al., 2001), assuming a elliptical form. Production of nauplii was estimated in the using empirical growth rate (Hirst and Bunker, 2003). The heterotrophic nanoflagellates (HNF) were collected in the surface layer. The carbon biomass of HNF was obtained from their count according to conversion factor described in Menden-Deuer and Lessard (2000). The biomass of ciliates was not recorded in 2008 and was therefore considered to be equal to 9.4 ± 3.3% of HNF biomass as was previously measured in the region at the same period (Vaqué et al., 2008). Microzooplankton diet was determined by grazing experiments in a previous study (Vaqué et al., 2008). The minimum herbivory-detritivory rate was estimated assuming that bacterial ingestion represents only 14% of the total ingestion of ciliates and HNF (Vaqué et al., 2008).

2.2.3.5. Mesozooplankton. Mesozooplankton was sampled using plankton nets with a 200 µm mesh size deployed vertically from 10 m above the bottom to the surface. Abundance was converted into carbon biomass using specific carbon-prosome length equation from Forest et al., (2011a) for the three dominant Arctic copepod species (*C. glacialis, C. hyperboreus* and *Metridia longa*). For other mesozooplankton species, the abundance was converted into carbon following the weight species-specific relation described in Hopcroft et al. (2005), assuming a carbon content of 50%. Mesozooplankton production was estimated by the product of its carbon biomasses and empirical growth rate, that is considered to be a function of chl *a*

concentration, surface temperature and body mass in carbon of each stage/species (Hirst and Bunker, 2003). Herbivory rates of the dominant copepods were estimated by measurement of chl *a* gut concentration using the gut fluorescence technique (Hattori and Saito, 1997).

2.2.3.6. Arctic cod larvae. The biomass of Arctic cod larvae was estimated using hydroacoustic methods. Acoustic data at 38 and 120 kHz were continuously recorded on ship (Geoffroy et al., 2015). In parallel, age 0 and age 1 fish were sampled to validate the acoustical signal. The collected data were processed with the same protocol using Echoview 5.3. The top 13.5 m of the water column and the last meter above the seafloor were excluded from the analysis. Data were analyzed in order to avoid the possible detection of zooplankton and larger fish living in the sampling area. Owing to the vertical segregation of Arctic cod individuals within the water column according to their size, the acoustic data was averaged over 50 m layers from the surface to the bottom. Total length and body weight of cod larvae were estimated according to empirical formulae described in Geoffroy et al. (2015). Arctic cod larvae were located in the first hundred meters of the water column.

In order to constrain inflows and outflows of arctic cod, the consumption and the respiration have to be limited by realistic values. There is a gap in metabolism data for *young of the year* Arctic cod (Thanassekos and Fortier, 2012). We made allometric extrapolations from experiments on juveniles. Respiration values came from Hop and Graham (1995), who measured the respiration of juvenile cod under two different conditions: (1) starvation and (2) after feeding *ad libitum*. Under starved conditions, they measured basal metabolism. On the contrary, under food-saturated conditions, the loss of energy increased and they measured active metabolism. Oxygen demand is greater following a feeding event than during the locomotive activity associated with hunting (Soofiani and Hawkins, 1982). The respiration after feeding was therefore considered as maximum possible respiration. Both measures of respiration were adjusted to the body mass of the larvae following the allometric formula described in Hop and Graham (1995), converted in terms of carbon with a conversion factor of 0.309 mg C per mg O_2 (Brey et al., 2010).

Minimum consumption was set to the maintenance daily ration expressed in g of wet body weight (Hop et al., 1997). The maximal daily ration of Amundsen Gulf cod larvae was determined using the following allometric relationship (Hop et al., 1997).

$$\log(C) = 0.7138\log(W) + 1.5272 \quad (2)$$

C refers to the consumption in mg per day and W to the wet body weight (g). The consumption was first converted in kJ using the mean energy content of prey consumed by the Arctic cod in Hop et al.'s experiments. Then the kJ was converted to carbon using the conversion factor of 45.7 J mg C^{-1} (Brey, 2001).

The minimal and maximal body mass of the 0–50 and 50–100 m layers were used to determine both the minimal and maximal individual respiration and consumption rates for each layer. The minimal and maximal individual daily consumption and respiration rates were multiplied by the mean abundance in each layer during the period under consideration and by the number of days in the period to obtain the limits of consumption and respiration for the entire study period. Eventually, the values in each layer were summed to obtain the consumption and respiration in the first 100 m and then integrated into the model as lower and upper values of soft constraints of respiration and consumption.

2.2.3.7. Diet of arctic cod larvae. The composition of Arctic cod larvae diet was determined using gut content analysis. Each prey was identified to the lowest taxonomical level possible. Prosome length for copepods and total length for other taxa were measured in order to estimate the carbon content of each prey using carbon-length relationships (for more details see Bouchard et al., 2014). Species were grouped according to the five compartments of micro and mesozooplankton defined in the model and their contribution to the total consumption of the larvae was calculated. The 5th and 95th percentiles were used as minimal and maximal bounds of contribution of each compartment to the larvae's diet.

2.2.4. Sensitivity analysis

Sensitivity analysis is used to determine the impact of the information integrated into the model on the whole set of flows values. The aim is to simulate the absence of information on particular processes (one flow or a sum of flows) and its impact on the estimation of all the other flow values. We chose to successively delete the complete information (i.e. lower and upper limits) relating to the process, by removing the set of soft constraints constraining this process. Thus, the process was no longer directly constrained but remained constrained by mass balances.

As a starting point, however, the mass balances and hard constraints relative to phytoplankton primary production were kept in every simulation. Soft constraints (i.e. biological constraints) could be divided into three groups according to their origin: (1) soft constraints from field measurements that were specific to the considered ecosystem, (2) soft constraints from allometric relationships that were adapted to the considered ecosystem by the use of body masses and biomass measured *in situ* and (3) soft constraints corresponding to metabolic rates, such as the assimilation efficiency. These constraints are applicable and true for all ecosystems, with the exception of bacterial growth efficiency (BGE), which varies according to the ecosystem considered. Considering that soft constraints related to metabolic rates (type 3) will always be present, regardless of the ecosystem being considered, they were left unchanged in the sensitivity analysis (except BGE), while only soft constraints of type 1 and 2 were successively removed (Table 1). This approach led to 36 models, each representing the same food web and with the same topology, but containing different sets of constraints. In the rest of the manuscript these models are called altered models and are referenced by the numbers provided in Table 1.

First each model was submitted to the LIM-MCMC approach to estimate all flow values. The LIM-MCMC uses a point (a value for a flow fulfilling all constraints) to determine a second point from a normal distribution centered on the first point, which has a fixed standard deviation, which corresponds to the jump. 20,000 iterations and a jump of 10 $gC{\cdot}m^{-2}$ were chosen to examine the entire solution space. We used a MATLAB routine implemented by Vézina and Campo and derived from the R-CRAN project package limSolve (Van den Meersche et al., 2009).

Network analysis of each simulated food web model obtained by LIM-MCMC was then computed in order to describe the functioning of the entire ecosystem emerge from flows values. Ecological Network Analysis (ENA) indices are known to be powerful tools to discriminate between different ecosystems or different states of a same ecosystem (Dame and Christian, 2007) and thus are appropriate for distinguishing the food web properties of each of the 36 altered models. A set of 9 broadly used indices was analyzed in this study in order to get an overall view of the food web features (see Fig. 2 for schematic representation of the different indices). The most of them, called Network ENA, analyze the organisation and the structure of the network in order to determine how a carbon atom flows through it. The total system throughput (T..) estimates the total quantity of carbon flowing through the food web (sum of all flows). The average mutual information (AMI) measures how much the carbon is constrained within the whole food web. As the Ascendency (A) is the product between AMI and T.., it estimates both the intensity of activity and the level of organisation within the ecosystem. The relative Ascendency (AC) evaluates the level of ecosystem activity and organisation relative to the maximum level attainable. The combination of the Finn Cycling Index (FCI), which estimates the relative quantity of cycling carbon (i.e. involved in loops)

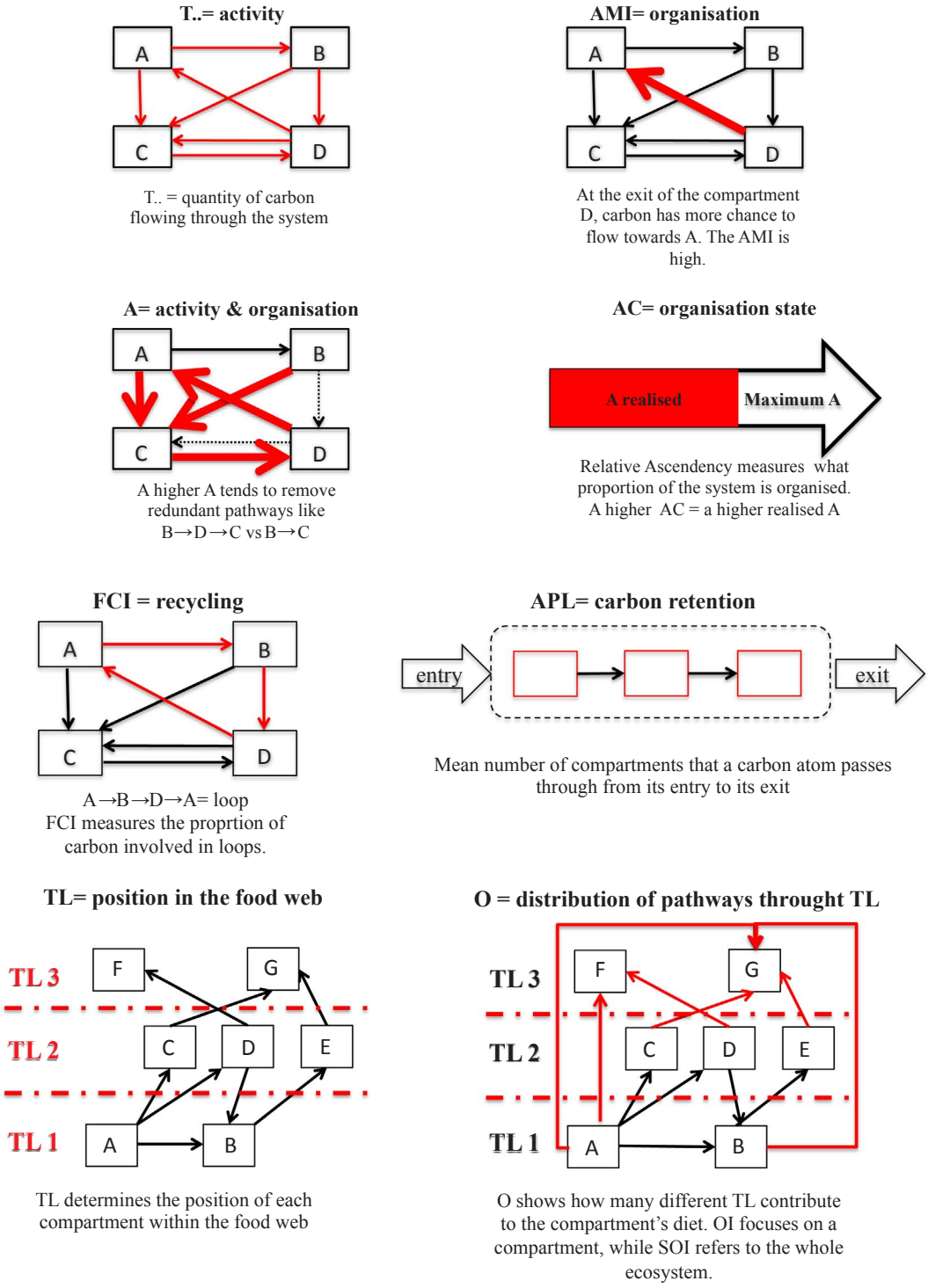
T..= activity
A
B
C
D
T.. = quantity of carbon flowing through the system
AMI= organisation
At the exit of the compartment D, carbon has more chance to flow towards A. The AMI is high.
A= activity & organisation
A higher A tends to remove redundant pathways like B→D→C vs B→C
AC= organisation state
A realised
Maximum A
Relative Ascendency measures what proportion of the system is organised. A higher AC = a higher realised A
FCI = recycling
A→B→D→A= loop
FCI measures the proprtion of carbon involved in loops.
APL= carbon retention
entry
exit
Mean number of compartments that a carbon atom passes through from its entry to its exit
TL= position in the food web
TL 3
TL 2
TL 1
F
G
C
D
E
A
B
TL determines the position of each compartment within the food web
O = distribution of pathways throught TL
O shows how many different TL contribute to the compartment's diet. OI focuses on a compartment, while SOI refers to the whole ecosystem.

Fig. 2. Schematic description of the nine ENA indices used in this paper. A, B, C and D represent compartments and arrows represent carbon pathways. Arrows point out the sink compartment. Red indicates what is measured by each index, the dotted arrows represent eliminated pathways. T.. = Total System Throughput, AMI = Average Mutual Information, A = Ascendency, Ac = Relative Ascendency, FCI = Finn's Cycling Index, APL = Average Path Length, TL = Trophic Level, O = Omnivory (OI = Omnivory Index and SOI = System Omnivory Index). (For interpretation of the references to colour in this figure legend, the reader is referred to the web version of this article.)

and the Average Path Length (APL) measuring the retention of carbon, gives a comprehensive view of the carbon recycling within the ecosystem. Diet_ENA are complementary indices that go into details about the consumption and diet proportions of each compartment. The trophic level provides information about the position of a particular compartment in the food web from both its diet composition and the trophic level of its prey. Omnivory measures how much a specific compartment (OI) or all compartments (SOI) feed on several trophic

levels and thus provides information on the distribution of trophic interaction through trophic levels. The SOI corresponds to the average OI of all compartments weighted by their own ingestion (Christensen et al., 2005).

ENA indices for which the calculation details are available in Latham (2006), were calculated using the R-CRAN project package NetIndices (Kones et al., 2009). A set of ENA indices was calculated for each set of flow solutions (20,000) and this for each of the altered model and the reference model.

2.3. Change in information and consequences for the food web

Alteration of the process information integrated to the different models was supposed to affect food web at two levels: (1) on the values of flows estimated by the LIM and (2) on the food web emergent properties. The results obtained for each altered model were then analyzed and compared to the reference model containing the complete set of soft constraints (i.e. complete information) on process, with the aim of highlighting differences at these two levels. In the first case, the comparison was based on the sets of mean flow values obtained from all models. The similarity of altered models with the reference models was analyzed using the Taylor diagram. It is a powerful tool for model comparison based on three points, that allows (1) describing the similarity of data via the calculation of correlation coefficient, (2) quantifying the difference between models using the root mean square (RMS) and (3) comparing the variability observed in each model by the calculation of standard deviation. The Taylor diagram was then completed by linear regression and an ANCOVA model in order to determine which altered model was significantly different from the reference model. To finish, the cumulative absolute error on flow allowed quantifying the total error caused by the removal of specific constraint. The cumulative difference highlighted the balance between over- and under-estimation.

The mean value, 5th and 95th percentile were calculated for all Network ENA indices and for the System Omnivory Index (SOI) of the reference model. For altered models, the mean value of each ENA indices was calculated and their position in comparison to the reference distribution was analyzed for each model.

For others Diet ENA indices, the mean trophic level and mean omnivory index for each compartment and for each model including the reference were calculated. The values obtained were represented on two radar plots in order to obviously visualize the impact of altered model on the trophic levels (or the omnivory indices) of all compartments.

3. Results

3.1. Comparison of flow values

All models showed a correlation coefficient greater than 0.9, suggesting a high similarity of all models with the reference one (Fig. 3). The RMS quantified a difference less than 2 $gC{\cdot}m^{-2}$ for almost all altered models. The standard deviation, that quantifies the dispersion of flow values observed in each model, presented similar or very close values for altered and reference models. This set of parameters allows concluding that almost altered models are similar to the reference one. The two models 14 (removal of the bacterial growth efficiency information) and 15 (removal of bacterial exudation information) stand out according to their relatively higher RMS, lower correlation coefficients and lower standard deviations, meaning a smaller variation in values. Only three other models could be distinguished from the reference model to a much lesser extent: the models 6 (information of bacterial production removed), 9 (removal of herbivory of *C. hyperboreus* information) and 12 (information on the sum of microzooplankton herbivory/detritivory was deleted).

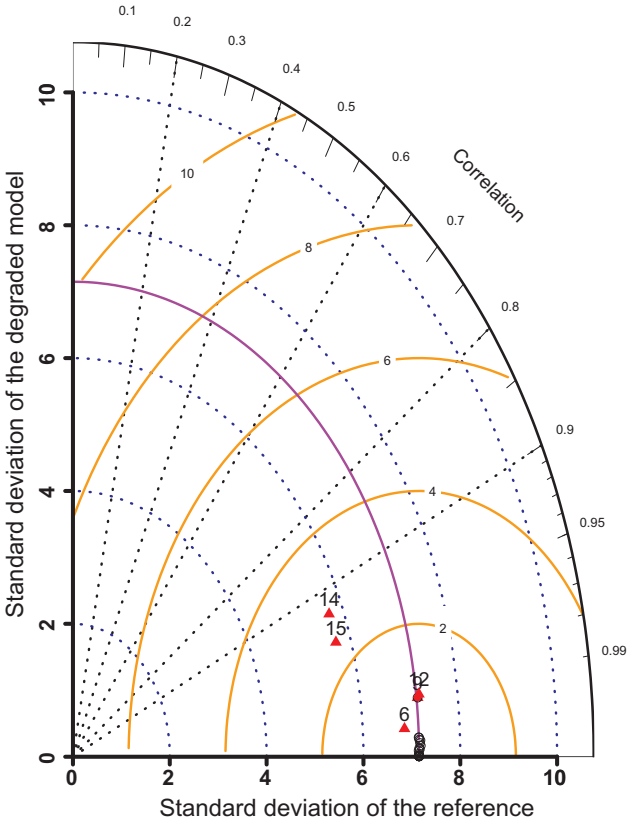

Fig. 3. Taylor diagram showing three aspects of model intercomparison: the correlation, the root mean square (RMS) and the standard deviation of each model. The circular edge (black) marks the correlation coefficient between the reference and an altered model. Orange arcs illustrate the RMS that quantifies the actual difference between the reference and an altered model. The x and y axes show the standard deviation of the reference and altered models, respectively. The purple arc represents the standard deviation of the reference model. Models are placed on the diagram according to the values of these three parameters (correlation coefficient, standard deviation and RMS). Dots that are placed close to both the bottom edge and the purple arc, are the most similar to the reference model. The empty black circles represent altered models similar to the reference one. Red triangles show altered models presenting clear differences with the reference model. (For interpretation of the references to colour in this figure legend, the reader is referred to the web version of this article.)

The regression lines of almost altered models (including the 9th and 12th) overlap the theoretical perfect one (Fig. 4). This suggests that model 9 and 12 are not significantly different from the reference model. The intercepts for models 14 (removal of bacterial growth efficiency) and 15 (bacterial exudation was removed) are significantly different from 0 ($a = 0.87$ and $a = 0.63$, respectively) and their slopes (both very close to 0.75) are significantly different from 1. The regression line of model 6 (information of bacterial production removed) has a slope slightly (but not significantly) different from the perfect regression line and an intercept value similar to the perfect regression line. Thus only the models 14 and 15 appear significantly different from the reference model.

Looking at the cumulative differences between the values of each flow (Fig. 5), virtually no differences were observed between the altered models and the reference from the 16th model onward. The majority of the sums of absolute values of the differences remained

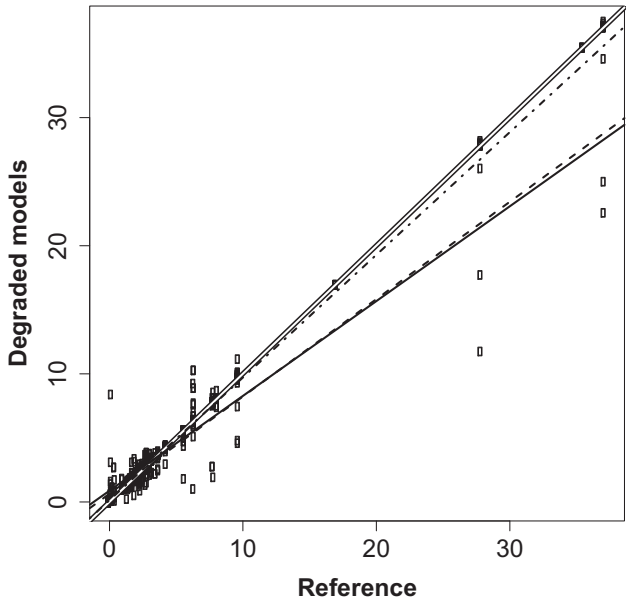

Fig. 4. Linear regression of the mean flow values ($gC{\cdot}m^{-2}{\cdot}summer^{-1}$) from the 36 altered models with those from the reference model. Each dot corresponds to a flow value. The regression line of almost all models and the theoretical perfect regression line (intercept = 0 and slope = 1) overlap (white line edged black). Models 6 (dotdashed), 14 (solid black) and 15 (dashed) shows a regression line different from the perfect one.

below 20 $gC{\cdot}m^{-2}{\cdot}summer^{-1}$, except for models 14 (bacterial growth efficiency information was removed) and 15 (bacterial exudation information was deleted), which presented maximums above 50 $gC{\cdot}m^{-2}{\cdot}summer^{-1}$. With the exception of models 12 (removal of the information on the sum of microzooplankton herbivory/detritivory), 14 and 15, the sum of differences (taking into account the sign of the difference) presented values close to zero that expressed the compensatory effect occurring between the various fluxes within the trophic network.

3.2. Comparison of ENA values

In this section, ENA indices are used to detect potential difference between the altered models and the reference model, because they synthesize information on flows magnitude into emerging organisation and functioning properties of the ecosystem. ENA indices affected by the same altered model were grouped together. Two pools of ENA were distinguished: the Network ENA indices based on flows magnitude only and the Diet ENA indices based on the consumption and diet of each compartment.

Network_ENA indices describe how a carbon atom flows within the boundaries of the ecosystem and are calculated from the set of flow values. All indices showed the same trend, with only two or three models (always the same) presenting ENA index values outside of the 5th or 95th percentile of their distribution (Fig. 6).

Model 15 (removal of the constraints on the bacterial exudation) presented the lowest values for all indices. The mean total system throughput (T..) was significantly lower for models 12 (removal of the information on the microzooplankton herbivory/detritivory), 14 (constraints on the bacterial growth efficiency was removed) and 15. This suggests less carbon flowing through the ecosystem. The significant drop of Average Mutual Information (AMI) for the models 14 and 15, suggests that an atom of carbon has a lower chance to pass through a particular pathway at the exit of a compartment (see Fig. 2). The product of T.. and AMI, called Ascendency (A), showed a significant decrease in the organisation and the size of the system for models 12, 14 and 15. The efficient and organised part of the food web estimated by the relative ascendency (AC), decreased from about 40% for the reference to about 35% for models 14 and 15 but remained unchanged for the model 12. The recycling index (FCI) also decreased for models 12 and 15 but on the contrary increased for model 14. This indicates that a greater proportion of carbon in the system was involved in a loop in model 14 than in all the other models. However, as evidenced by their lower Average Path length (APL) values, a carbon atom seemed to spend less time within the trophic networks of models 12, 14 and 15.

The Diet_ENA indices are based on the consumption of each compartment and the proportion that different prey each represent in their diet. These ENA indices are complementary to the Network_ENA indices because they provide more detail about trophic relationships, focusing

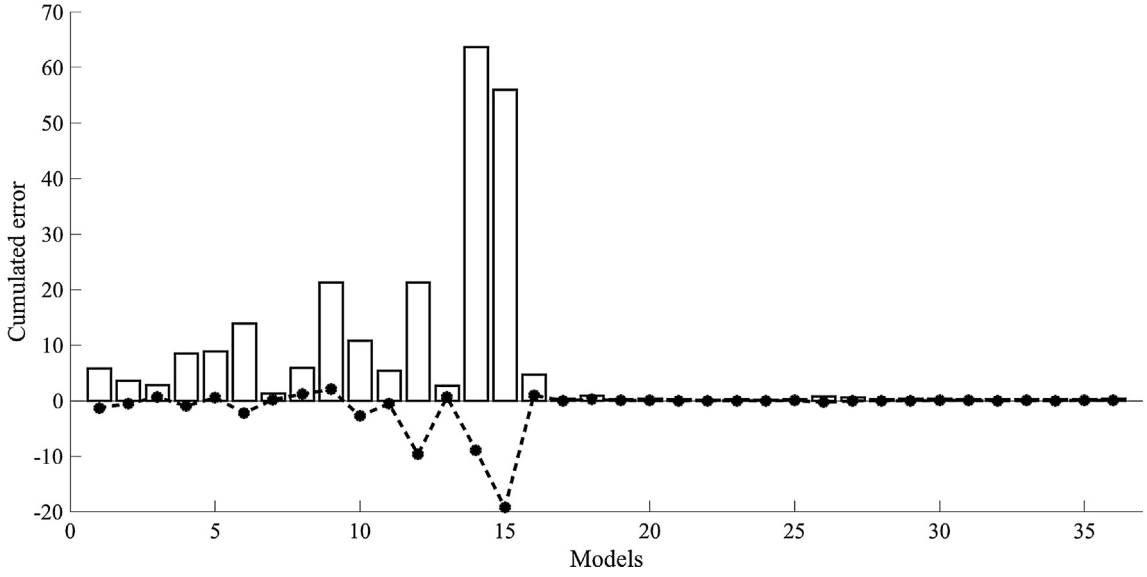

Fig. 5. Cumulative differences between each altered model (identified by number) and the reference. The bars represent the sum of the absolute values of differences for each flow. The dashed line represents the actual sum of differences for each model; here the sign of the difference is considered.

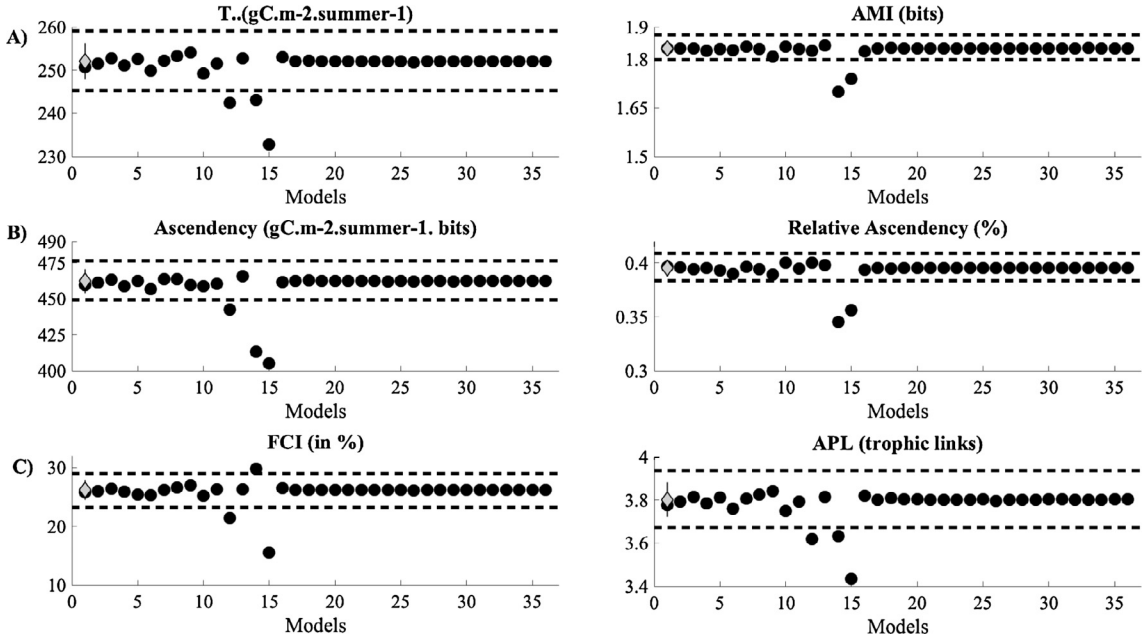

Fig. 6. Values of selected Network ENA indices. The grey diamonds represent the values for the reference model with their standard deviations. The black dots show the mean value of indices from the ensemble of 20,000 ENA values for each altered model. The dashed lines represent the 5th and 95th percentiles of the distribution of reference calculated from its ensemble of 20,000 ENA values. (A) presents indices describing the size and the organisation of the system, (B) corresponds to indices determining the state of organisation and (C) shows indices estimating the cycling and the retention of carbon.

on the source of carbon ingested (i.e. originating from a different trophic level), the number of food sources for a predator and the relative proportion of an individual source in the total carbon ingested by each predator. The trophic level and omnivory index are defined for each compartment of the food web (Fig. 6). Indices for primary producers, detritus and bacteria are not represented because their values are always constant. By convention, the trophic level of primary producers and detritus is fixed at 1 and that of bacteria is fixed at 2. These compartments present an null omnivory index because primary producers and detritus do not feed and bacteria feed on a single resource, detritus.

The same compartments were affected for both trophic levels and omnivory index, regardless of the model under consideration, suggesting a relationship between omnivory index and trophic level (Fig. 7). Models 5 (constraints on the microzooplankton production were removed), 9 (removal of *C. hyperboreus* production), 11 (bacterivory by microzooplankton was deleted) and 12 (the removal of the constraints on the sum of microzooplankton herbivory/detritivory) present values of trophic level and omnivory index different from the reference model for several compartments (Fig. 7).

The trophic levels and omnivory indices increased for models 5 (the removal of constraints on the microzooplankton production), 9 (constraints on the *C. hyperboreus* production was removed) and 12 (information on the microzooplankton herbivory/detritivory was deleted) the trophic levels and the omnivory indices were greater than the reference model (Fig. 7). On the contrary model 11 (information of

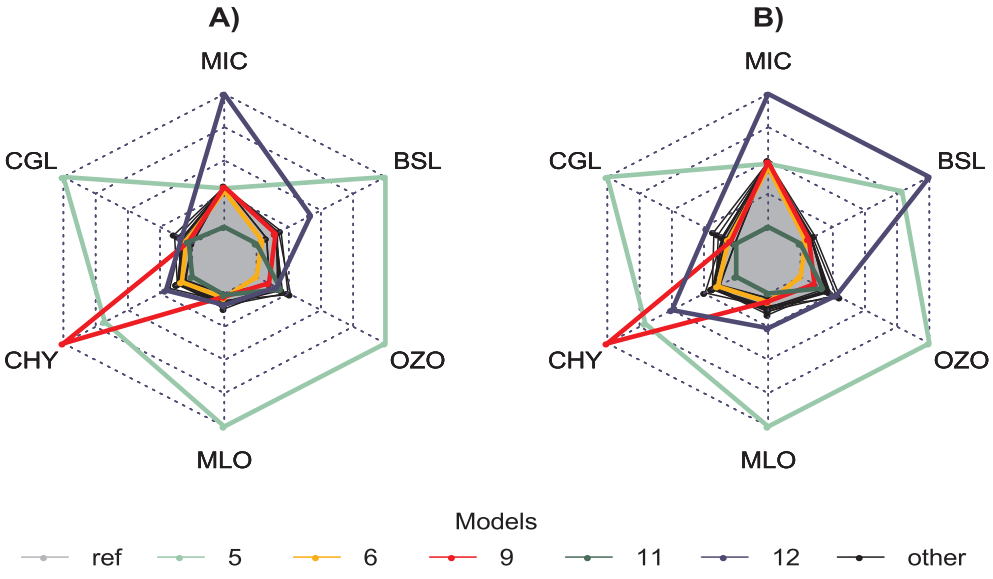

Fig. 7. Radar plot presenting: (A) the trophic levels of each compartment and (B) the omnivory index of each compartment, represented by the different axes. MIC = microzooplankton, BSL = *Boreogadus saida* larvae, OZO = other zooplankton, MLO = *Metridia longa*, CHY = *Calanus hyperboreus*, CGL = *Calanus glacialis*. The grey surface corresponds to the space defined by the values for the reference model. To draw the radar plot we considered the minimum and maximum for the trophic levels and omnivory indices of all models, including the reference. The minimal values are in the center of the radar plot, while the maximum values were at the edge. Each dot was drawn according to its value compared to the previously determined minimum and the maximum. Dots placed far from the grey surface present a strong difference from the reference values.

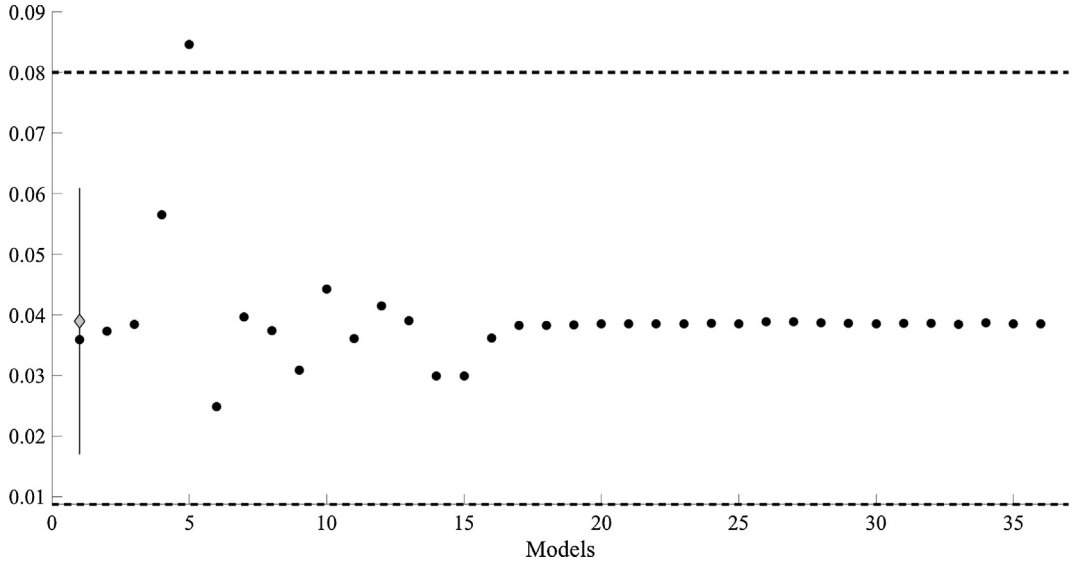

Fig. 8. Omnivory Index for the entire ecosystem. The grey diamonds represent the values for the reference model with their standard deviations. The black dots show the mean value of indices from the ensemble of 20,000 ENA values for each altered model. The dashed lines represent the 5th and 95th percentiles of the distribution of the reference model calculated from its ensemble of 20,000 ENA values.

bacterivory by microzooplankton was deleted) presented trophic levels and omnivory indices were lower than the reference model. In model 5, trophic levels and omnivory indices increased for all compartments, with the exception of microzooplankton. Whereas, in model 12, the microzooplankton trophic level increased and, to a lesser extent, so did those of Arctic cod (*B. saida*) larvae and the large copepod *C. hyperboreus*. The increase in the omnivory index for the latter was higher than the increase in their trophic levels. Model 9 led to an increase of the trophic level of *C. hyperboreus* only. On the contrary, model 11 presented a decrease in the trophic levels and omnivory indices of *C. hyperboreus*, Arctic cod larvae and microzooplankton.

The system omnivory index (SOI) estimates mean omnivory for the entire ecosystem and thus allows us determine if the difference observed for each altered model at the compartment scale (Fig. 8) was still observed at the ecosystem scale. From model 16 onward, the SOI was identical to that of the reference model. For the others models, the SOI value remained in the range of the standard deviation of the reference model (Fig. 7). Only model 5 (removal of constraints on microzooplankton production) presented a SOI value above the 95th percentile of the distribution range of the reference model values. It was twice as high as the reference value, indicating that species feed on a higher proportion of prey from different trophic levels in this model.

4. Discussion

We analyzed the effects of removing specific information in a simulated Arctic food web and assessed the magnitude of the carbon flows and their ecological implications on the ecosystem emergent properties based on calculation of ENA indices. When only flow values were considered, just two models were seemed significantly different from the reference model. After ENA indices revealed further differences, the two groups of ENA indices that we computed (Network_ENA and Diet_ENA indices) were not sensitive to the same constraints.

4.1. Robustness of Amundsen Gulf food web model to available information

Overall, the food web model for the Amundsen Gulf was robust. Only two altered models were significantly different from the reference model (Figs. 3 and 4): model 14, where the direct constraints on bacterial growth efficiency were relaxed (i.e. removed) and model 15, where the direct constraints on bacterial exudation were relaxed. In this model, the flow of bacteria to dissolved organic carbon considered the excretion of metabolites like polysaccharides by bacteria, and the viral lysis. However, the mean flow values from both models were strongly correlated with the reference model ($R > 90\%$). This shows that despite the observed localized differences, the food web as a whole remains very similar to the reference model.

This robustness can first be explained by the fact that flows are not limited by a unique constraint. A flow is usually constrained in three ways: (i) by direct constraints referring to absolute values of its magnitude range (those relaxed in our sensitivity analysis), (ii) by a combination of constraints limiting its relative magnitude compared to other flows and (iii) indirectly by mass balance constraints on the set of flows of a particular compartment. Complex interactions between constraints limit the value of an individual flow, preventing it from taking on an unrealistic value. This demonstrates that the food web model is well designed since it allows for flexibility in the computation of flow values but offers no flexibility for aberrant values.

The topology of the food web, particularly the number of effective trophic links measured by the connectance (i.e. number of links/the number of possible links), can explain this surprising robustness. Indeed, the Arctic food web present a high connectance ($C = 0.40$) compared to other food webs ($C < 0.315$ for 16 food webs around the world in (Dunne et al., 2002)). Thus, a change in the magnitude of a process is distributed over several trophic links, limiting the apparition of large errors and non-realistic values. For instance, the excess of the microzooplankton production observed in the model 5 was distributed to the 5 predation flows, thus limiting the impact on the entire simulated food web. As a consequence, the impact on ecosystem properties emerging from flow values is limited.

4.2. Robustness of Ecological Network Analysis indices

In this study, we distinguished two groups of ENA indices: (i)

Network_ENA, which describe how a carbon atom flows through the food web and (ii) Diet_ENA, which estimate the distribution of the trophic pathways across the trophic levels (Vasconcellos et al., 1997). Both groups of ENA indices responded differently to the relaxation of constraints, each expressing contrasting aspects of the trophic network response.

The effect of removing constraints on the sum of flows controlled the impact on Network ENA (see models 12, 14 and 15 Figs. 4 and 5). The models where the cumulative differences in flows were close to zero (dashed line in Fig. 4), suggesting a compensation effect between under- and over-estimations of individual flows and thus an unchanged sum of flows, did not show any noticeable modifications of their Network_ENA indices. Kones et al. (2009) showed that since ENA indices are calculated from combinations of flows, they are more robust than single flows. Significant changes in the Network_ENA values became evident when the relaxation of some information did not lead to a strong enough compensation effect among other flows.

Diet_ENA indices did not follow the same patterns. Compartment scale indices were sensitive to smaller changes in the food web since they were based on the relative proportion of each resource in a predator's diet. The total amount of food ingested by a predator could remain unchanged while the diet composition changed drastically. At a higher level of organisation, the system omnivory index was more robust, with changes observed in only one model. In fact, effects at the compartment scale must be strong enough and impact several consumers compartments in order to generate a cumulative impact on the omnivory of the whole ecosystem.

4.3. Ecological interpretation of the sensitivity analysis

In the reference model, the bacterial carbon available for higher trophic level was controlled by 2 elements: (i) bacterial growth efficiency, which defines the efficiency at which bacteria produce particulate carbon from their uptake of dissolved carbon, and (ii) exudation, including viral lysis. Bacterial growth efficiency was removed in model 14, whereas exudation was removed in model 15. Despite a decrease in dissolved carbon uptake, the balance between both of these processes led to an increase in the quantity of bacterial carbon available. Indeed, model 14 increased bacterial growth efficiency and viral lysis, while both processes were increased by model 15 (see Appendix Table A3). The consequences for the emergent properties at the ecosystem level are similar, except for recycling. In model 14, a large part of the new particulate carbon returned to the dissolved carbon compartment via viral lysis. This created a loop between bacteria and dissolved carbon compartments that increased the recycling within the ecosystem, as measured by the cycling index (FCI, Fig. 6). In model 15, the quantity of carbon involved in the bacteria-dissolved carbon loop decreased in response to the decrease in uptake and exudation. However, in both models the higher bacterial production was exported and lost, instead of being ingested by the higher trophic levels (i.e. bacterivory remained the same as the reference model). The decrease in the average path length value (APL) confirmed that an atom of carbon spent less time within the food web.

This also highlighted a less efficient transfer of carbon within the ecosystem as a whole, shown by the decrease in the Relative Ascendency (AC). The relative Ascendency, that represents the efficient and organised part of the ecosystem, is associated to the resistance of the ecosystem. The relative overheads, defined as 1-AC, constitute the reserves of the ecosystem, the part that is not organised yet and bring flexibility and thus resilience to the ecosystem. To be stable, an ecosystem must present a balance between resistance and resilience (Ulanowicz et al., 2009). The reference model presented an almost perfect balance between resistance and resilience, indicating an optimal exploitation and transfer of the resources available within the ecosystem (AC = 40%, Overheads = 60%). Both altered models caused a decrease in the resistance due to a reduced transfer of carbon from dissolved carbon to bacteria. As a consequence, the energy (carbon) available within the system was not fully exploited and the non-exploited dissolved organic carbon was lost from the ecosystem via export.

Model 12 was the only model to show concurrent changes in both the Network_ and Diet_ENA indices. In the reference model, microzooplankton fed on phytoplankton (19%), detritus (65%) and bacteria (16%). Removing the constraints on the consumption of phytoplankton and detritus by microzooplankton caused a decrease in detritivory (to 37% Table A3). The relative proportions of the different food sources ingested by microzooplankton changed and bacteria became its main prey (39%). Because bacteria are at a higher trophic level than detritus, the trophic level of microzooplankton subsequently increased. Moreover, the more uniform predation by microzooplankton on its three prey categories caused an increase in its omnivory index as well. Despite a decrease in its consumption, microzooplankton production remained the same (implying a decrease in its egestion and respiration, see Table A3) and thus did not impact the carbon transfer to its predators and their diet. Thus, the increasing omnivory index observed for the consumers of microzooplankton (Fig. 7) was not due to an actual change in their own diets, but to the increase in the microzooplankton trophic level further along in the process. Since changes in flows remained limited to flows to and from the detritus compartment, the rest of the food web remained almost unchanged and ecosystem functioning was only slightly affected. Carbon was efficiently transferred through particular trophic pathways from one compartment to another (i.e. similar AMI and AC). However, the decrease in detritivory and egestion by microzooplankton led to less carbon in the detritus-microzooplankton loop (i.e. recycling decreased, Fig. 6). This, combined with an increase in the loss of detritus by export (about 160% Table A3), caused a decrease in the carbon retention within the ecosystem in model 12.

The relaxation of the information on microzooplankton production in model 5 only impacted Diet_ENA indices. First, it resulted in an increase of microzooplankton production (Table A1). This excess of production was transferred to higher trophic levels, but without affecting their total consumption. As a consequence, the mesozooplankton consumed more microzooplankton and less phytoplankton compared to the reference model (Table A3). In this altered model, mesozooplankton fed on fresh organic carbon from the primary production and recycled organic carbon via the microbial loop (phytoplankton → dissolved carbon → bacteria → microzooplankton). The overall available carbon is also well distributed through the different pathways, allowing it to be fully exploited. This change in mesozooplankton diet increased their trophic levels since they fed on a higher proportion of prey from higher trophic positions, leading to an amplification effect from the lower to the upper trophic levels. Moreover, concurrent changes in trophic level and diet composition caused an increase in the omnivory index for microzooplankton consumers (Fig. 6). The synergistic effect of these increases of compartmental omnivory, coupled with the static ingestion levels of microzooplankton predators increased the omnivory index of the entire ecosystem (Fig. 7). This increase in the ecosystem omnivory index demonstrated how the redistribution of carbon through the existing pathways permitted a better exploitation of available energy.

4.4. Process that should be better documented

From a methodological point of view, Diet ENA reveals changes that are not visible with an analysis solely limited to flow differences because of their high sensitivity to changes in relative proportion among consumption flows. Diet_ENA indices may therefore be a good tool for monitoring Arctic ecosystem currently facing unprecedented anthropogenic pressure and environmental changes. Indeed, the survey of the trophic level and omnivory index permits an early detection of potentially larger changes in the organisation and functioning of the ecosystem, which subsequently allows ecosystem management policies to be adapted more quickly. Trophic level is already used in ecosystem management because of its ease of *in situ* measurements via isotopic approaches (Coll et al., 2016; Cury et al., 2005). Omnivory is currently used to estimate the quality of an ecosystem. A survey of omnivory trends highlights the level of stress that an ecosystem faces, be it anthropogenic pressure (Selleslagh et al., 2012) or environmental stress like eutrophication (Patrício and Marques, 2006). In an ecosystem that becomes disturbed, predators become more opportunistic and thus, omnivory tends to increase.

In this study, change in the system omnivory index was only observed when the microzooplankton was consumed in higher proportions, while the phytoplankton remained available. The validity of this scenario has to be demonstrated. The predation of microzooplankton by copepods, reported in different ecosystems around the world, is not related to phytoplankton concentration (Levinsen et al., 2000), but can be linked to the high nutritional quality of microzooplankton (Broglio et al., 2003; Stoecker and Capuzzo, 1990), the high probability of encounter (Calbet and Saiz, 2005) or the optimal microzooplankton size range. In this model, microzooplankton included copepods nauplii. Cannibalism or intraguild predation by different species of copepods has been already reported in cases of low phytoplankton availability. The proportion of the diet represented by eggs depends on the species being considered. However, it is linked to the probability of encounter between adults and eggs or young nauplii stages as shown in Basedow and Tande (2006) and Dufour et al. (2016).

Climate change threatens phytoplankton grazing by copepods because of the potential mismatch between the timing of phytoplankton bloom and the upward migration of the copepods from diapause (Leu et al., 2011; SØReide et al., 2010). Another threat is the apparent change in phytoplankton communities, from the large phytoplantonic cells (e.g. diatoms, dinoflagellates), favoured by copepods, to picophytoplankton, which are at the lower end of the size range for their preferred prey (Li et al., 2009). Grazing on microzooplankton appears to be an alternate strategy to ensure copepod growth. Monitoring trophic levels and omnivory of copepods in the Arctic Ocean may help determine whether copepod diet preferences are shifting towards microzooplankton, therefore indicating a possible reorganization of the pelagic food web well before dramatic changes in community composition, biodiversity or biomass are detectable.

From an ecological point of view, this study clearly showed the impact of bacterial processes on the functioning of the entire ecosystem. Bacteria affect carbon cycling and carbon retention, due to their ability to incorporate dissolved organic carbon (not exploitable otherwise) into new particulate carbon that can be transferred towards the higher trophic levels, as well as their ability to remineralize organic detritus that restock the nutrient pool (Rivkin and Legendre, 2001; Rivkin and Legendre, 2002). Moreover, bacteria represent an alternative food source for microzooplankton and hence an indirect resource for higher trophic levels. Because bacteria are essential in the regulation of the functioning of the Arctic marine ecosystems, it is essential to collect *in situ* information on the two major processes controlling bacterial production, namely: (i) bacterial growth efficiency (Del Giorgio and Cole, 2000) and (ii) the contribution of bacteria to dissolved organic pool via the excretion of metabolites and viral lysis. As shown in this study, missing or inaccurate information about these processes impacts the estimation of the total quantity of carbon flowing within the boundaries of the ecosystem as well as the quantity of carbon potentially produced by bacteria that could be transferred to higher trophic levels.

Bacterial Growth Efficiency (BGE) determines the balance between catabolic (i.e. loss of carbon via respiration) and anabolic (i.e. creation of new biomass) activities (Del Giorgio and Cole, 2000). Higher BGE means lower loss of carbon by respiration and higher particulate carbon production. The BGE was first thought as an inverse function of temperature (Rivkin and Legendre, 2001), but the interaction between temperature and the concentration of dissolved carbon in the control of bacterial growth was then shown to be important (Kirchman et al., 2005; Kirchman et al., 2009b; Ortega-Retuerta et al., 2012). BGE values measured *in situ* in the Arctic Ocean are variable and contrasted depending on ecosystem and season, ranging from less than 10% to more than 20% (e.g. Meon and Amon, 2004; Sherr and Sherr, 2003). In our model, BGE settled around 24%, very close to the upper prescribed boundary (Forest et al., 2011b). The BGE in Amundsen Gulf was estimated to be a maximum of 18.6% during the summer period (Nguyen et al., 2012). The bacterial efficiency was probably overestimated in the model and thus bacterial carbon production as well. An understanding of the fine controls of dissolved organic carbon and by temperature on bacterial growth is essential for predicting the effects of environmental changes on bacteria and, consequently, the entire ecosystem (Kirchman et al., 2009b).

Although the role of bacteria as generator of organic carbon was ignored for a long time, it is nowadays accepted that their contribution is about 25% of the dissolved and particulate carbon pools (Kaiser and Benner, 2008). Bacteria produce dissolved carbon via two processes: viral lysis (see below), and excretion of diverse metabolites during their growth (del Giorgio and Cole, 1998) such as exoenzymes (to degrade particular carbon), mucilaginous protective capsules (Azam et al., 1999), etc.. Dissolved products can represent up to 25% of bacterial respiration (Stoderegger and Herndl, 2001), and 14–31% of total bacterial carbon production. However, the current methods used to measure bacterial production are based on the intracellular carbon concentration and thus do not integrate the production of DOC. As a consequence, the bacterial production and BGE are most probably underestimated (Kawasaki and Benner, 2006). Moreover, the dissolved bacterial products are refractory (i.e. resistant to the microbial degradation) and thus contribute to carbon sequestration. There is a growing number of studies considering this process as part of the new microbial carbon pump concept (Jiao et al., 2010, 2011). For these reasons, it is essential to have an accurate understanding and assessment of these microbial processes for a robust representation of food webs (Gasol et al., 2008).

Viral lysis of bacteria likely plays an important, but still uncertain role, in the transfer of carbon through the food web and the biogeochemical cycle, but quantifying its impact is difficult (Suttle, 2007). Viral lysis shunts the transfer of carbon to the higher trophic levels, transforming bacteria to dissolved and largely unconsumed particulate carbon. Usually, viral lysis represents from 10 to 40% of bacterial mortality (Weinbauer et al., 2002). In Arctic waters, the relative importance of viral lysis compared to microzooplankton grazing depends on depth (Comiso, 2012; Steward et al., 1996) and season (Boras et al., 2010; Yager et al., 2001). The impacts of accelerating warming in the Arctic, especially ice melting, is expected to decrease bacterial viral infection due to increasing competition from heterotrophic protists

(Boras et al., 2010). As a consequence, a higher proportion of bacterial carbon would be transferred to higher trophic levels to the detriment of flux to dissolved and particulate organic carbon. A good description and understanding of the viral lysis process is crucial for providing an accurate description of the Arctic marine ecosystem functioning.

5. Conclusion

ENA indices appear to be a powerful tool for highlighting changes in the food web that are not visible by simple monitoring of biomass or flow values. On one hand, changes in bacterial growth efficiency or loss of dissolved carbon by bacteria (possibly via viral lysis) caused a disruption of the emergent properties of the ecosystem, affecting its state of resistance and resilience. Integrating accurate information about these elements in the food web model is crucial to efficiently understand and describe both the inner functioning and the stability of Arctic marine ecosystems. On the other hand, changes at the level of microzooplankton led to significant changes in the diet of higher trophic level consumers. Monitoring the mesozooplankton trophic level would be the best strategy for surveying the state of Arctic food web as it could be the "canary in a coal mine" that we need to anticipate possible tipping points in these fragile ecosystems that are currently facing risks unprecedented in recent history.

6. Perspectives

Despite its sensitivity to some soft constraints, our model ended up being surprisingly robust. The robustness of our food web model likely emerged from the strong connectivity between the compartments. As a result, food webs presenting a similar topology should present a similar robustness to alteration of soft constraint, even outside of the Arctic region. A future sensitivity analysis on a food web model whose connectivity patterns are altered (instead of its soft constraints) should be realized to test this conclusion.

The conclusion that the Amundsen Gulf planktonic ecosystem is sensitive to the information available on bacterial growth efficiency and bacterial excretion of dissolved carbon (including viral lysis), could be relevant for other marine ecosystems of the world. The issue of the availability of bacterial carbon to the higher trophic level is prevalent in most marine ecosystems (Kirchman et al., 2009a). As a result, when designing a new trophic network study for any marine ecosystem, our results clearly indicate that the bacterial compartment and its production dynamics should not be overlooked. In absence of relevant information, efforts should be dedicated to the measurements of bacterial processes controlling the availability of carbon to higher trophic levels.

We showed that the fate of the bacterial production via the microzooplankton within the trophic network could be monitored through the variability of the trophic position of mesozooplankton. Microzooplankton serves as a hub between the microbial and classical food webs in all marine ecosystems, and higher transfer of microzooplankton carbon to the higher trophic levels implies a higher indirect ingestion of heterotrophic bacteria. Thus, monitoring the trophic level of mesozooplankton appeared as a simple and efficient way to (i) detect potential changes in the lower trophic levels and (ii) test the usefulness of the homologous ENA index to detect these changes. Hence, we recommend adding this measurement to the suite of variables routinely measured in studies of trophic networks from any marine ecosystems.

Finally, this study highlighted heterotrophic processes that shape the distribution of carbon through the trophic pathways. Considering another currency for the trophic network analysis, such as nitrogen, could reveal a different functioning and different critical processes in the marine ecosystem under study. Such an approach in trophic network modeling could eventually help bridging the gap between the ecological conclusions obtain from trophic network analysis and biogeochemical models of marine ecosystems whose elemental currency is essentially nitrogen.

To conclude, this paper led the way to improve our representation of marine ecosystem functioning and to determine more powerful sentinel metrics, hopefully allowing better ecosystem management.

Acknowledgments

We gratefully thank C. Bouchard, M. Goeffroy and M. Leblanc for their support on the description of Arctic cod features in the Amundsen Gulf. BSB received a postdoctorate fellowship from the Canada Excellence Research Chair (CERC) in Remote Sensing of Canada's New Arctic Frontier (MB). This work benefited from a CRSNG Discovery Grant to FM. This is a contribution to the research programs of Québec-Océan, ArcticNet and UMI Takuvik.

Appendix A

See Fig. A1.

In this example, gpp (gross primary production) is the unique input in the food web model. Therefore it determines the quantity of carbon available in the food web. Carbon flows through the food web until it is definitively lost by respiration or export. The LIM-MCMC method aims at determining the quantity of carbon flowing through each flow *1–6*.

a, b and c are food web compartments. a and b are live compartments (i.e. they respire) and c is a non-living compartment (detritus). Flows are symbolized by arrows from the source to the sink. The symbol corresponds to the respiration of living compartments.

Numbers in **blue** refer to knowledge (from *in situ* and literature sources) that allows to determine flow constraints.
Numbers in **red** refer to fixed values.
Numbers in **green** are values of flows estimated by the LIM-MCMC.
The hatched area corresponds to the solution space of flows.
The yellow star shows the value that is randomly sampled.

x represents the flows of the food web, **b** and **h** is a numerical vector containing the values of the biological constraints and **A** and **G** are matrices containing the coefficients of the biological constraints (Vézina, 1989). For instance, in the inequation: $1 * \text{flow1} + (-0.3) * \text{gpp} \leq 0$ the flows (**x**) are flow1 and gpp, the coefficients (composing **G**) are composed of 1 and -0.3 and **h** is equal to 0.

LIM model construction

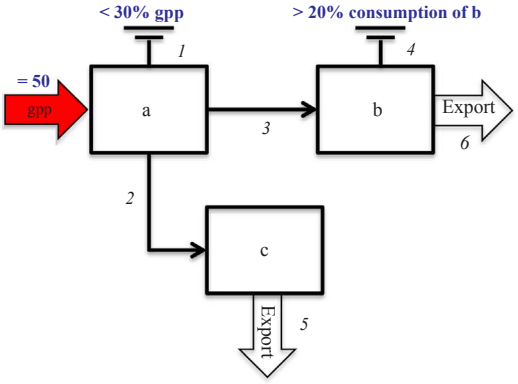

I. Linear equations (A*x=b)

I.1. Mass balance (inflows - outflows=0):

For a: 1*gpp + (- 1)*flow1 + (-1)* flow3 + (-1) flow2 = 0
For b: flow3 + (- 1)*flow4 + (- 1)*flow6 = 0
For c: flow2 + (- 1)*flow5 = 0

I.2. Flow fixed by a single value

gpp = 50

II. Linear inequalities (G*x ≤ h)

Flow1 ≤ 30%gpp → 1* flow1 + (-0.3)*gpp ≤ 0
Flow4 ≥ 20%consumption of b → (-1)*flow4 + 1* flow3 ≤ 0

LIM-MCMC solution space sampling

Gpp is integrated into the model asefixd value and serve as starting point.

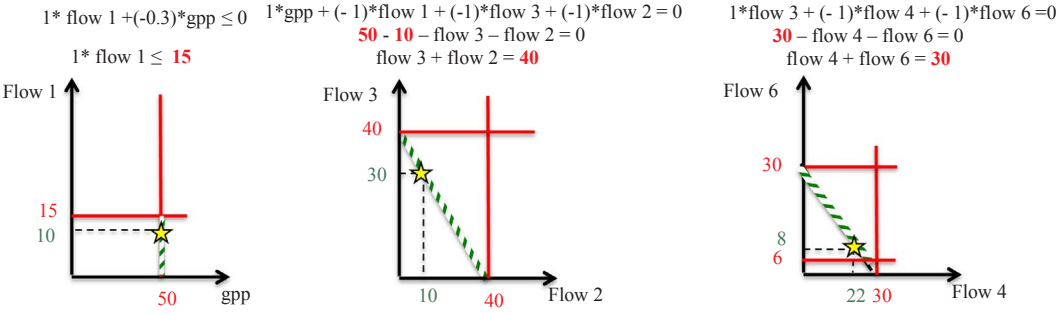

One of the possible resulting food web.

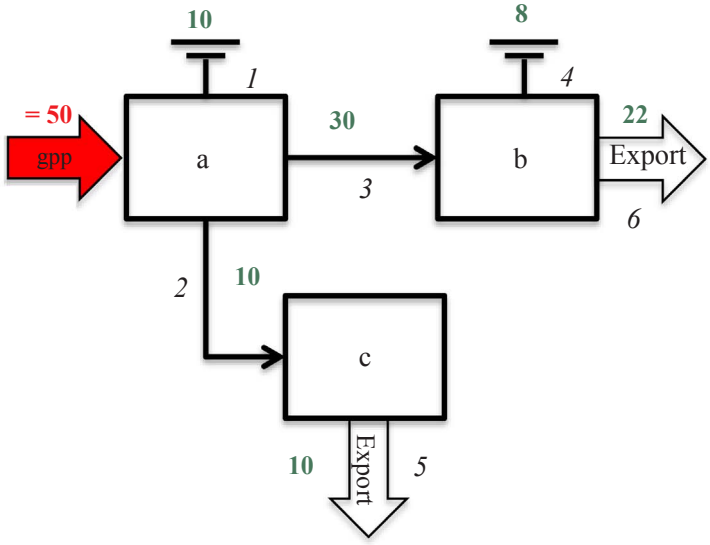

Fig. A1. Principle of the LIM method.

Table A1
List of the 65 flows integrated to the model.

Source of the flow	Sink of the flow
Gross primary production	Small phytoplankton
Gross primary production	Large phytoplankton
Small phytoplankton	Microzooplankton
	C. glacialis
	C. hyperboreus
	M. longa
	Other zooplankton
	Particulate detritus
	Dissolved detritus
	Respiration
Large phytoplankton	*C. glacialis*
	C. hyperboreus
	M. longa
	Other zooplankton
	Particulate detritus
	Dissolved detritus
	Respiration
Bacteria	Microzooplankton
	Other zooplankton
	Particulate detritus
	Dissolved detritus
	Respiration
	Export
Microzooplankton	*C. glacialis*
	C. hyperboreus
	M. longa
	Other zooplankton
	Arctic cod larvae
	Particulate detritus
	Dissolved detritus
	Respiration
	Export
C. glacialis	Arctic cod larvae
	Particulate detritus
	Dissolved detritus
	Respiration
	Export
C. hyperboreus	Arctic cod larvae
	Particulate detritus
	Dissolved detritus
	Respiration
	Export
M. longa	Arctic cod larvae
	Particulate detritus
	Dissolved detritus
	Respiration
	Export
Other zooplankton	Arctic cod larvae
	Particulate detritus
	Dissolved detritus
	Respiration
	Export
Arctic cod larvae	Particulate detritus
	Respiration
	Export
Particulate detritus	Microzooplankton
	C. Glacialis
	C. hyperboreus
	M. longa
	Other zooplankton
	Dissolved detritus
	Export
	Sedimentation
Dissolved detritus	Bacteria
	Export

Table A2
presents the model number associated with the constraints removed.

Number of altered models	Removal of the constraints on
1	*C. glacialis* production
2	M. longa production
3	*C. hyperboreus* production
4	Other zooplankton production
5	Microzooplankton production
6	Bacterial production
7	Herbivory by *C. glacialis*
8	Herbivory by *M. longa*
9	Herbivory by *C. hyperboreus*
10	Total respiration of mesozooplankton
11	Bacterivory by microzooplankton
12	Herbivory/detritivory by microzooplankton
13	Degradation of particulate carbon to dissolved carbon
14	Bacterial growth efficiency
15	Exudation including viral lysis
16	Sedimentation of particulate carbon
17	Arctic cod larvae respiration
18	Arctic cod larvae consumption
19	Predation of *C. glacialis* by Arctic cod larvae
20	Predation of *C. hyperboreus* by Arctic cod larvae
21	Predation of *M. longa* by Arctic cod larvae
22	Predation of other zooplankton by Arctic cod larvae
23	Predation of microzooplankton by Arctic cod larvae
24	Net carbon production
25	Maximum respiration of *C. glacialis*
26	Maximum respiration of *C. hyperboreus*
27	Maximum respiration of *M. longa*
28	Maximum respiration of other zooplankton
29	Maximum respiration of microzooplankton
30	Maximum respiration of bacteria
31	Maximum consumption by *C. glacialis*
32	Maximum consumption by *C. hyperboreus*
33	Maximum consumption by *M. longa*
34	Maximum consumption by other zooplankton
35	Maximum consumption by microzooplankton
36	Maximum uptake of DOC by bacteria

Table A3
Flows are expressed in $gC{\cdot}m^{-2}$ over the summer period.

	Models				
	Reference	5	12	14	15
Production					
SPH	17	17	17	17	17
LPH	35.5	35.5	35.5	35.5	35.5
BAC	2.866	2.865	2.912	3.952	3.779
MIC	1.258	3.865	1.134	1.262	1.261
CGL	1.499	1.500	1.578	1.739	1.731
MLO	1.628	1.632	1.728	1.914	1.911
CHY	1.704	1.710	1.709	1.720	1.720
OZO	1.823	1.813	1.911	2.126	2.116
BSL	0.033	0.033	0.033	0.033	0.033
Respiration					
SPH	1.032	1.024	1.129	1.876	1.807
LPH	1.965	1.961	2.080	3.412	3.199
BAC	27.879	27.865	28.245	11.800	17.770
MIC	2.778	2.792	1.368	3.753	3.730
CGL	2.062	2.106	2.128	2.411	2.385
MLO	2.484	2.514	2.495	2.675	2.669
CHY	3.269	3.251	3.274	3.401	3.394
OZO	2.312	2.255	2.409	2.995	2.958
BSL	0.008	0.008	0.008	0.008	0.008
Egestion (flow to DET)					
SPH	2.274	2.331	2.330	2.366	2.364
LPH	6.394	6.668	5.156	8.929	8.939
BAC	0.476	0.423	0.400	0.933	0.851
MIC	5.659	4.401	1.832	4.781	4.765

(*continued on next page*)

Table A3 (*continued*)

	Models				
	Reference	5	12	14	15
CGL	2.216	2.292	2.305	2.544	2.536
MLO	2.671	2.777	2.742	2.905	2.913
CHY	3.522	3.590	3.521	3.574	3.552
OZO	2.557	2.563	2.685	3.044	3.033
BSL	0.030	0.029	0.029	0.029	0.029
SUM	25.799	25.074	21.001	29.104	28.981
Exudation (flow to DOC)					
SPH	3.735	3.741	4.026	2.498	2.605
LPH	9.697	10.061	11.210	4.642	4.836
BAC	6.363	6.362	6.401	9.295	1.066
MIC	2.391	1.893	0.924	2.407	2.435
CGL	1.374	1.420	1.422	1.492	1.500
MLO	1.700	1.761	1.719	1.697	1.717
CHY	2.370	2.391	2.376	2.241	2.265
OZO	1.536	1.526	1.616	1.770	1.780
DET	8.132	8.120	8.171	7.441	7.559
SUM	37.299	37.275	37.865	33.483	25.763
Consumption					
BAC	37.109	26.047	27.047	25.047	22.615
MIC	12.086	12.951	5.257	12.202	12.191
CGL	7.150	7.318	7.432	8.187	8.152
MLO	8.483	8.685	8.684	9.190	9.210
CHY	10.865	10.943	10.880	10.937	10.930
OZO	8.228	8.157	8.620	9.935	9.886
BSL	0.071	0.070	0.070	0.071	0.070
Proportion of herbivory					
MIC	0.19	0.18	0.24	0.19	0.20
CGL	0.55	0.53	0.53	0.49	0.49
MLO	0.76	0.72	0.74	0.72	0.72
CHY	0.94	0.93	0.94	0.94	0.94
OZO	0.55	0.49	0.54	0.56	0.56
Proportion of detritivory					
MIC	0.65	0.66	0.37	0.64	0.64
CGL	0.40	0.30	0.43	0.48	0.48
MLO	0.21	0.17	0.23	0.25	0.25
CHY	0.04	0.04	0.04	0.04	0.04
OZO	0.38	0.33	0.40	0.39	0.39
Proportion of bacterivory					
MIC	0.16	0.16	0.39	0.16	0.16
OZO	0.03	0.03	0.03	0.03	0.03
Proportion of carnivory					
CGL	0.04	0.16	0.04	0.03	0.03
MLO	0.03	0.11	0.03	0.03	0.03
CHY	0.02	0.03	0.02	0.02	0.02
OZO	0.04	0.15	0.03	0.03	0.03
Export					
BAC	0.160	0.147	0.197	0.686	0.612
MIC	0.131	0.174	0.158	0.246	0.243
CGL	1.481	1.482	1.561	1.722	1.714
MLO	1.617	1.621	1.717	1.903	1.900
CHY	1.686	1.692	1.691	1.702	1.702
OZO	1.806	1.796	1.893	2.108	2.099
BSL	0.033	0.033	0.033	0.033	0.033
DET	0.190	0.184	0.305	1.646	1.448
DOC	0.190	0.184	0.307	8.436	3.148
Sedimentation					
DET	1.387	1.381	1.475	1.657	1.653

* For heterotrophic compartments, the production (P) is defined as P-C-R-E-e with C = Ingestion, R = Respiration, E = Egestion and e = exudation. Bacterial production as considered in the BGE formula, corresponds to BP = C-R.

References

Ardyna, M., Babin, M., Gosselin, M., Devred, E., Rainville, L., Tremblay, J.-É., 2014. Recent Arctic Ocean sea ice loss triggers novel fall phytoplankton blooms. Geophys. Res. Lett. 41, 6207–6212.

Arrigo, K.R., van Dijken, G., Pabi, S., 2008. Impact of a shrinking Arctic ice cover on marine primary production. Geophys. Res. Lett. 35.

Ayers, M.J., Scharler, U.M., Fennessy, S.T., 2013. Modelling ecosystem effects of reduced prawn recruitment on the Thukela Bank trawling grounds, South Africa, following

nursery loss. Mar. Ecol. Prog. Ser. 479, 143–161.
Baird, D., Asmus, H., Asmus, R., 2007. Trophic dynamics of eight intertidal communities of the Sylt-Rømø Bight ecosystem, northern Wadden Sea. Mar. Ecol. Prog. Ser. 351, 25–41.
Barber, D., Asplin, M., Gratton, Y., Lukovich, J., Galley, R., Raddatz, R., Leitch, D., 2010. The International Polar Year (IPY) Circumpolar Flaw Lead (CFL) system study: overview and the physical system. Atmos. Ocean 48, 225–243.
Basedow, S.L., Tande, K.S., 2006. Cannibalism by female Calanus finmarchicus on naupliar stages. Mar. Ecol. Prog. Ser. 327, 247–255.
Beaugrand, G., Kirby, R.R., 2010. Climate, plankton and cod. Glob. Change Biol. 16, 1268–1280.
Boras, J.A., Sala, M.M., Arrieta, J.M., Sà, E.L., Felipe, J., Agustí, S., Duarte, C.M., Vaqué, D., 2010. Effect of ice melting on bacterial carbon fluxes channelled by viruses and protists in the Arctic Ocean. Polar Biol. 33, 1695–1707.
Bouchard, C., Mollard, S., Suzuki, K., Robert, D., Fortier, L., 2014. Contrasting the early life histories of sympatric Arctic gadids Boreogadus saida and Arctogadus glacialis in the Canadian Beaufort Sea. Polar Biol. 39, 1005–1022.
Breed, G.A., Jackson, G.A., Richardson, T.L., 2004. Sedimentation, carbon export and food web structure in the Mississippi River plume described by inverse analysis. Mar. Ecol. Prog. Ser. 278, 35–51.
Brey, T., 2001. Population Dynamics in Benthic Invertebrates. A Virtual Handbook. Alfred Wegener Institute for Polar and Marine Research, Germany. http://www.awi-bremerhaven.de/Benthic/Ecosystem/FoodWeb/Handbook/main.html.
Brey, T., Müller-Wiegmann, C., Zittier, Z.M.C., Hagen, W., 2010. Body composition in aquatic organisms—a global data bank of relationships between mass, elemental composition and energy content. J. Sea Res. 64, 334–340.
Broglio, E., Jónasdóttir, S.H., Calbet, A., Jakobsen, H.H., Saiz, E., 2003. Effect of heterotrophic versus autotrophic food on feeding and reproduction of the calanoid copepod Acartia tonsa: relationship with prey fatty acid composition. Aquat. Microb. Ecol. 31, 267–278.
Calbet, A., Saiz, E., 2005. The ciliate-copepod link in marine ecosystems. Aquat. Microb. Ecol. 38, 157–167.
Carstensen, J., Conley, D.J., Bonsdorff, E., Gustafsson, B.G., Hietanen, S., Janas, U., Jilbert, T., Maximov, A., Norkko, A., Norkko, J., Reed, D.C., Slomp, C.P., Timmermann, K., Voss, M., 2014. Hypoxia in the Baltic Sea: Biogeochemical Cycles, Benthic Fauna, and Management. AMBIO 43, 26–36.
Christensen, V., Walters, C.J., Pauly, D., 2005. Ecopath with Ecosim: A User's Guide. Fisheries Centre, University of British Columbia, Vancouver, pp. 154.
Chrystal, R.A., Scharler, U.M., 2014. Network analysis indices reflect extreme hydrodynamic conditions in a shallow estuarine lake (Lake St Lucia), South Africa. Ecol. Ind. 38, 130–140.
Coll, M., Shannon, L.J., Kleisner, K.M., Juan-Jordá, M.J., Bundy, A., Akoglu, A.G., Banaru, D., Boldt, J.L., Borges, M.F., Cook, A., Diallo, I., Fu, C., Fox, C., Gascuel, D., Gurney, L.J., Hattab, T., Heymans, J.J., Jouffre, D., Knight, B.R., Kucukavsar, S., Large, S.I., Lynam, C., Machias, A., Marshall, K.N., Masski, H., Ojaveer, H., Piroddi, C., Tam, J., Thiao, D., Thiaw, M., Torres, M.A., Travers-Trolet, M., Tsagarakis, K., Tuck, I., van der Meeren, G.I., Yemane, D., Zador, S.G., Shin, Y.J., 2016. Ecological indicators to capture the effects of fishing on biodiversity and conservation status of marine ecosystems. Ecol. Ind. 60, 947–962.
Comiso, J.C., 2012. Large decadal decline of the arctic multiyear ice cover. J. Clim. 25, 1176–1193.
Cury, P.M., Shannon, L.J., Roux, J.P., Daskalov, G.M., Jarre, A., Moloney, C.L., Pauly, D., 2005. Trophodynamic indicators for an ecosystem approach to fisheries. ICES J. Mar. Sci. 62, 430–442.
Daly, K.L., 1997. Flux of particulate matter through copepods in the Northeast water polynya. J. Mar. Syst. 10, 319–342.
Dame, J., Christian, R., 2007. A statistical test of network analysis: can it detect differences in food web properties? Ecosystems 10, 906–923.
Darnis, G., Robert, D., Pomerleau, C., Link, H., Archambault, P., Nelson, R.J., Geoffroy, M., Tremblay, J.-É., Lovejoy, C., Ferguson, S.H., Hunt, B.P.V., Fortier, L., 2012. Current state and trends in Canadian Arctic marine ecosystems: II. Heterotrophic food web, pelagic-benthic coupling, and biodiversity. Clim. Change 115, 179–205.
del Giorgio, P.A., Cole, J.J., 1998. Bacterial growth efficiency in natural aquatic systems. Annu. Rev. Ecol. Syst. 29, 503–541.
Del Giorgio, P., Cole, J., 2000. Bacterial energetics and growth efficiency. Microbial Ecol. Oceans 289–325.
Dufour, K., Maps, F., Plourde, S., Joly, P., Cyr, F., 2016. Impacts of intraguild predation on arctic copepod communities. Front. Mar. Sci. 3, 185.
Dugdale, R.C., Goering, J.J., 1967. Uptake of new and regenerated forms of nitrogen in primary productivity. Limnol. Oceanogr. 12, 196–206.
Dunne, J.A., Williams, R.J., Martinez, N.D., 2002. Food-web structure and network theory: the role of connectance and size. Proc. Natl. Acad. Sci. 99, 12917–12922.
Elton, C. (Ed.), 1927. Animal Ecology. Sidgwick & Jackson, London.
Forest, A., Galindo, V., Darnis, G., Pineault, S., Lalande, C., Tremblay, J.E., Fortier, L., 2011a. Carbon biomass, elemental ratios (C:N) and stable isotopic composition (13C, 15N) of dominant calanoid copepods during the winter-to-summer transition in the Amundsen Gulf (Arctic Ocean). J. Plankton Res. 33, 161–178.
Forest, A., Tremblay, J.-É., Gratton, Y., Martin, J., Gagnon, J., Darnis, G., Sampei, M., Fortier, L., Ardyna, M., Gosselin, M., Hattori, H., Nguyen, D., Maranger, R., Vaqué, D., Marrasé, C., Pedrós-Alió, C., Sallon, A., Michel, C., Kellogg, C., Deming, J., Shadwick, E., Thomas, H., Link, H., Archambault, P., Piepenburg, D., 2011b. Biogenic carbon flows through the planktonic food web of the Amundsen Gulf (Arctic Ocean): a synthesis of field measurements and inverse modeling analyses. Prog. Oceanogr. 91, 410–436.
Frangoulis, C., Carlotti, F., Eisenhauer, L., Zervoudaki, S., 2010. Converting copepod vital rates into units appropriate for biogeochemical models. Prog. Oceanogr. 84, 43–51.
Garneau, M.-È., Roy, S., Lovejoy, C., Gratton, Y., Vincent, W.F., 2008. Seasonal dynamics of bacterial biomass and production in a coastal arctic ecosystem: Franklin Bay, western Canadian Arctic. J. Geophys. Res. 113.
Gasol, J.M., Pinhassi, J., Alonso-Sáez, L., Ducklow, H., Herndl, G.J., Koblízek, M., Labrenz, M., Luo, Y., Morán, X.A.G., Reinthaler, T., Simon, M., 2008. Towards a better understanding of microbial carbon flux in the sea*. Aquat. Microb. Ecol. 53, 21–38.
Gaston, A.J., Woo, K., Hipfner, J.M., 2003. Trends in forage fish populations in northern Hudson Bay since 1981, as determined from the diet of nestling thick-billed murres Uria lomvia. Arctic 227–233.
Geoffroy, M., Majewski, A., LeBlanc, M., Gauthier, S., Walkusz, W., Reist, J.D., Fortier, L., 2015. Vertical segregation of age-0 and age-1+ polar cod (Boreogadus saida) over the annual cycle in the Canadian Beaufort Sea. Polar Biol. 39, 1023–1037.
Gosselin, M., Levasseur, M., Wheeler, P.A., Horner, R.A., Booth, B.C., 1997. New measurements of phytoplankton and ice algal production in the Arctic Ocean. Deep Sea Res. Part II 44, 1623–1644.
Hattori, H., Saito, H., 1997. Diel changes in vertical distribution and feeding activity of copepods in ice-covered Resolute Passage, Canadian Arctic, in spring 1992. J. Mar. Syst. 11, 205–219 %@ 0924-7963.
Hirst, A.G., Bunker, A.J., 2003. Growth of marine planktonic copepods: Global rates and patterns in relation to chlorophyll a, temperature, and body weight. Limnol. Oceanogr. 48, 1988–2010.
Hop, H., Graham, M., 1995. Respiration of juvenile Arctic cod (Boreogadus saida): effects of acclimation, temperature, and food intake. Polar Biol. 15, 359–367.
Hop, H., Tonn, W.M., Welch, H.E., 1997. Bioenergetics of Arctic cod (Boreogadus saida) at low temperatures. Can. J. Fish. Aquat. Sci. 54, 1772–1784.
Hopcroft, R.R., Clarke, C., Nelson, R.J., Raskoff, K.A., 2005. Zooplankton communities of the Arctic's Canada Basin: the contribution by smaller taxa. Polar Biol. 28, 198–206.
Jiao, N., Herndl, G.J., Hansell, D.A., Benner, R., Kattner, G., Wilhelm, S.W., Kirchman, D.L., Weinbauer, M.G., Luo, T., Chen, F., Azam, F., 2010. Microbial production of recalcitrant dissolved organic matter: long-term carbon storage in the global ocean. Nat. Rev. Microbiol. 8, 593.
Jiao, N., Herndl, G.J., Hansell, D.A., Benner, R., Kattner, G., Wilhelm, S.W., Kirchman, D.L., Weinbauer, M.G., Luo, T., Chen, F., Azam, F., 2011. The microbial carbon pump and the oceanic recalcitrant dissolved organic matter pool. Nat. Rev. Microbiol. 9, 555.
Kaiser, K., Benner, R., 2008. Major bacterial contribution to the ocean reservoir of detrital organic carbon and nitrogen. Limnol. Oceanogr. 53, 99–112.
Kawasaki, N., Benner, R., 2006. Bacterial release of dissolved organic matter during cell growth and decline: Molecular origin and composition. Limnol. Oceanogr. 51, 2170–2180.
Kirchman, D.L., Malmstrom, R.R., Cottrell, M.T., 2005. Control of bacterial growth by temperature and organic matter in the Western Arctic. Deep Sea Res. Part II 52, 3386–3395.
Kirchman, D.L., Moran, X.A.G., Ducklow, H., 2009a. Microbial growth in the polar oceans – role of temperature and potential impact of climate change. Nat. Rev. Microbiol. 7, 451–459.
Kirchman, D.L., Moran, X.A.G., Ducklow, H., 2009b. Microbial growth in the polar oceans role of temperature and potential impact of climate change. Nat. Rev. Microbiol. 7, 451–459.
Klein, B., LeBlanc, B., Mei, Z.-P., Beret, R., Michaud, J., Mundy, C.J., von Quillfeldt, C.H., Garneau, M.-È., Roy, S., Gratton, Y., Cochran, J.K., Bélanger, S., Larouche, P., Pakulski, J.D., Rivkin, R.B., Legendre, L., 2002. Phytoplankton biomass, production and potential export in the North Water. Deep Sea Res. Part II 49, 4983–5002.
Kones, J.K., Soetaert, K., van Oevelen, D., Owino, J.O., 2009. Are network indices robust indicators of food web functioning? A Monte Carlo approach. Ecol. Model. 220, 370–382.
Kwok, R., Rothrock, D., 2009. Decline in Arctic sea ice thickness from submarine and ICESat records: 1958–2008. Geophys. Res. Lett. 36.
Latham, L.G., 2006. Network flow analysis algorithms. Ecol. Model. 192, 586–600.
Leu, E., Søreide, J.E., Hessen, D.O., Falk-Petersen, S., Berge, J., 2011. Consequences of changing sea-ice cover for primary and secondary producers in the European Arctic shelf seas: timing, quantity, and quality. Prog. Oceanogr. 90, 18–32.
Levinsen, H., Turner, J.T., Nielsen, T.G., Hansen, B.W., 2000. On the trophic coupling between protists and copepods in arctic marine ecosystems. Mar. Ecol. Prog. Ser. 204, 65–77.
Li, W.K., McLaughlin, F.A., Lovejoy, C., Carmack, E.C., 2009. Smallest algae thrive as the Arctic Ocean freshens. Science 326 539–539.
Link, J.S., Stockhausen, W.T., Methratta, E.T., 2005. Food-Web theory in marine ecosystems. In: Belgrano, A., Scharler, U.M., Dunne, J.A., Ulanowicz, R.E. (Eds.), Aquatic Food Webs An Ecosystem Approach. Oxford University Press, Oxford, pp. 98–113.
Loreau, M., 1994. Material cycling and the stability of ecosystems. Am. Natural. 143, 508–513.
Maps, F., Record, N.R., Pershing, A.J., 2013. A metabolic approach to dormancy in pelagic copepods helps explaining inter-and intra-specific variability in life-history strategies. J. Plankton Res. 18–30.
Marquis, E., Niquil, N., Delmas, D., Hartmann, H.J., Bonnet, D., Carlotti, F., Herbland, A., Labry, C., Sautour, B., Laborde, P., Vézina, A., Dupuy, C., 2007. Inverse analysis of the planktonic food web dynamics related to phytoplankton bloom development on the continental shelf of the Bay of Biscay, French coast. Estuar. Coast. Shelf Sci. 73, 223–235.
Menden-Deuer, S., Lessard, E.J., 2000. Carbon to volume relationships for dinoflagellates, diatoms, and other protist plankton. Limnol. Oceanogr. 45, 569–579.
Meon, B., Amon, R.M., 2004. Heterotrophic bacterial activity and fluxes of dissolved free amino acids and glucose in the Arctic rivers Ob, Yenisei and the adjacent Kara Sea. Aquat. Microb. Ecol. 37, 121–135.

Moloney, C.L., Field, J.G., 1989. General allometric equations for rates of nutrient uptake, ingestion, and respiration in plankton organisms. Limnol. Oceanogr. 34, 1290–1299.
Naeem, S., Thompson, L.J., Lawler, S.P., Lawton, J.H., Woodfin, R.M., 1994. Declining biodiversity can alter the performance of ecosystems. Nature 368, 734–737.
Nguyen, D., Maranger, R., Tremblay, J.E., Gosselin, M., 2012. Respiration and bacterial carbon dynamics in the Amundsen Gulf, western Canadian Arctic. J. Geophys. Res.-Oceans 117.
Nozais, C., Gosselin, M., Michel, C., Tita, G., 2001. Abundance, biomass, composition and grazing impact of the sea-ice meiofauna in the North Water, northern Baffin Bay. Mar. Ecol. Prog. Ser. 217, 235–250.
Ortega-Retuerta, E., Jeffrey, W., Babin, M., Bélanger, S., Benner, R., Marie, D., Matsuoka, A., Raimbault, P., Joux, F., 2012. Carbon fluxes in the Canadian Arctic: patterns and drivers of bacterial abundance, production and respiration on the Beaufort Sea margin. Biogeosciences 9, 3679.
Patrício, J., Marques, J.C., 2006. Mass balanced models of the food web in three areas along a gradient of eutrophication symptoms in the south arm of the Mondego estuary (Portugal). Ecol. Model. 197, 21–34.
Pimm, S.L., 1984. The complexity and stability of ecosystems. Nature 307, 321–326.
Riemann, B., Carstensen, J., Dahl, K., Fossing, H., Hansen, J.W., Jakobsen, H.H., Josefson, A.B., Krause-Jensen, D., Markager, S., Stæhr, P.A., Timmermann, K., Windolf, J., Andersen, J.H., 2016. Recovery of Danish coastal ecosystems after reductions in nutrient loading: a holistic ecosystem approach. Estuaries Coasts 39, 82–97.
Rivkin, R.B., Legendre, L., 2001. Biogenic carbon cycling in the upper ocean: effects of microbial respiration. Science 291, 2398–2400.
Rivkin, R.B., Legendre, L., 2002. Roles of food web and heterotrophic microbial processes in upper ocean biogeochemistry: global patterns and processes. Ecol. Res. 17, 151–159.
Saint-Béat, B., Baird, D., Asmus, H., Asmus, R., Bacher, C., Pacella, S.R., Johnson, G.A., David, V., Vézina, A.F., Niquil, N., 2015. Trophic networks: how do theories link ecosystem structure and functioning to stability properties? A review. Ecol. Ind. 52, 458–471.
Savenkoff, C., Vézina, A.F., Smith, P.C., Han, G., 2001. Summer transports of nutrients in the Gulf of St. Lawrence estimated by inverse modelling. Estuar. Coast. Shelf Sci. 52, 565–587.
Selleslagh, J., Lobry, J., Amara, R., Brylinski, J.-M., Boët, P., 2012. Trophic functioning of coastal ecosystems along an anthropogenic pressure gradient: a French case study with emphasis on a small and low impacted estuary. Estuar. Coast. Shelf Sci. 112, 73–85.
Shadwick, E.H., Thomas, H., Chierici, M., Else, B., Fransson, A., Michel, C., Miller, L.A., Mucci, A., Niemi, A., Papakyriakou, T.N., Tremblay, J.É., 2011. Seasonal variability of the inorganic carbon system in the Amundsen Gulf region of the southeastern Beaufort Sea. Limnol. Oceanogr. 56, 303–322.
Sherr, B.F., Sherr, E.B., 2003. Community respiration/production and bacterial activity in the upper water column of the central Arctic Ocean. Deep Sea Res. Part I 50, 529–542.
Smith, D.C., Azam, F., 1992. A simple, economical method for measuring bacterial protein synthesis rates in seawater using 3H-leucine. Mar. Microb. Food Webs 6, 107–114.
Soofiani, N.M., Hawkins, A.D., 1982. Energetic costs at different levels of feeding in juvenile cod, Gadus morhua L. J. Fish Biol. 21, 577–592.
Søreide, J.E., Leu, E.V.A., Berge, J., Graeve, M., Falk-Petersen, S., 2010. Timing of blooms, algal food quality and Calanus glacialis reproduction and growth in a changing Arctic. Glob. Change Biol.
Steward, G.F., Smith, D.C., Azam, F., 1996. Abundance and production of bacteria and viruses in the Bering and Chukchi Seas. Mar. Ecol. Prog. Ser. 131, 287–300.
Stoderegger, K.E., Herndl, G.J., 2001. Visualization of the exopolysaccharide bacterial capsule and its distribution in oceanic environments. Aquat. Microb. Ecol. 26, 195–199.
Stoecker, D.K., Capuzzo, J.M., 1990. Predation on protozoa: its importance to zooplankton. J. Plankton Res. 12, 891–908.
Straile, D., 1997. Gross growth efficiencies of protozoan and metazoan zooplankton and their dependence on food concentration, predator-prey weight ratio, and taxonomic group. Limnol. Oceanogr. 42, 1375–1385.
Suttle, C.A., 2007. Marine viruses major players in the global ecosystem. Nat. Rev. Microbiol. 5, 801–812.
Thanassekos, S., Fortier, L., 2012. An Individual Based Model of Arctic cod (Boreogadus saida) early life in Arctic polynyas: I. Simulated growth in relation to hatch date in the Northeast Water (Greenland Sea) and the North Water (Baffin Bay). J. Mar. Syst. 93, 25–38.
Tremblay, J.-É., Michel, C., Hobson, K.A., Gosselin, M., Price, N.M., 2006. Bloom dynamics in early opening waters of the Arctic Ocean. Limnol. Oceanogr. 51, 900–912.
Ulanowicz, R.E., Goerner, S.J., Lietaer, B., Gomez, R., 2009. Quantifying sustainability: resilience, efficiency and the return of information theory. Ecol. Complex. 6, 27–36.
Van den Meersche, K., Soetaert, K., Van Oevelen, D., 2009. xsample ( ): an R function for sampling linear inverse problems. J. Stat. Softw. 30.
van Oevelen, D., Van den Meersche, K., Meysman, F.J.R., Soetaert, K., Middelburg, J.J., Vézina, A.F., 2010. Quantifying food web flows using linear inverse models. Ecosystems 13, 32–45.
Vaqué, D., Guadayol, Ò., Peters, F., Felipe, J., Angel-Ripoll, L., Terrado, R., Lovejoy, C., Pedrós-Alió, C., 2008. Seasonal changes in planktonic bacterivory rates under the ice-covered coastal Arctic Ocean. Limnol. Oceanogr. 53, 2427–2438.
Vasconcellos, M., Mackinson, S., Sloman, K., Pauly, D., 1997. The stability of trophic mass-balance models of marine ecosystems: a comparative analysis. Ecol. Model. 100, 125–134.
Vézina, A.F., 1989. Construction of flow networks using inverse methods. In: Network Analysis in Marine Ecology. Springer, pp. 62–81.
Vézina, A.F., Pace, M.L., 1994. An inverse model analysis of planktonic food webs in experimental lakes. Can. J. Fish. Aquat. Sci. 51, 2034–2044.
Vézina, A.F., Platt, T., 1988. Food web dynamics in the ocean. 1. Best-estimates of flow networks using inverse methods. Mar. Ecol. Progr. Ser. 42, 269–287.
Walsh, J.E., 2008. Climate of the Arctic marine environment. Ecol. Appl. 18.
Wassmann, P., Duarte, C.M., Agusti, S., Sejr, M.K., 2011. Footprints of climate change in the Arctic marine ecosystem. Glob. Change Biol. 17, 1235–1249.
Weinbauer, M.G., Winter, C., Höfle, M.G., 2002. Reconsidering transmission electron microscopy based estimates of viral infection of bacterio- plankton using conversion factors derived from natural communities. Aquat. Microb. Ecol. 27, 103–110.
Wilhelm, S.W., Suttle, C.A., 1999. Viruses and Nutrient Cycles in the Sea: viruses play critical roles in the structure and function of aquatic food webs. Bioscience 49, 781–788.
Yager, P.L., Connelly, T.L., Mortazavi, B., Wommack, K.E., Bano, N., Bauer, J.E., Opsahl, S., Hollibaugh, J.T., 2001. Dynamic bacterial and viral response to an algal bloom at subzero temperatures. Limnol. Oceanogr. 46, 790–801.